An-Najah National University

Faculty of Graduate Studies

THERMO-OXIDATIVE DECOMPOSITION ANALYSIS OF PALM WASTES BY ISOCONVERSIONAL KINETICS AND AMMONIA FIBER EXPANSION

By

Duha Abdalla Fathi Yousef

Supervisors

Dr. Ismail Badran

Dr. Derar Smadi

This Thesis is Submitted in Partial Fulfilment of the Requirements for the Degree of Master of Chemistry, Faculty of Graduate Studies, An-Najah National University, Nablus - Palestine.

2025

THERMO-OXIDATIVE DECOMPOSITION ANALYSIS OF PALM WASTES BY ISOCONVERSIONAL KINETICS AND AMMONIA FIBER EXPANSION

By

Duha Abdalla Fathi Yousef

This Thesis was Defended Successfully on 20/02/2025 and approved by

Dr. Ismail Badran Supervisor	Ismail Badran Signature
Dr. Derar Smadi Co Supervisor	Signature
Dr. Abedullah Eid External Examiner	Signature
Dr. Rawan Khalaf Internal Examiner	Signature

Dedication

I wholeheartedly dedicate this work to my greatest supporter and source of inspiration, my cherished mother, and to my dear father, whose love and guidance have always been a foundation of strength. To my wonderful siblings—Yassin, Yousef, Abd Al Rahman, and Aseel—your constant encouragement and unwavering presence have been invaluable.

I also extend this dedication to my devoted friends and extended family, whose support and motivation have been a source of strength throughout this journey.

With profound gratitude and respect, I thank you all for your unwavering belief in me.

Acknowledgements

I'd like to thank An-Najah University's Chemistry Department for their continual help and unflinching support in completing this thesis.

Many thanks to my supervisor, Dr. Ismail Badran, for his advice and unwavering support throughout my job. Also, I would like to thank Dr. Derar Smadi, the head of the Chemistry Department (co-supervisor), for his kindness in assisting me with my inquiries concerning my work. I'd also like to thank all the teaching staff in the Chemistry Department. As well as Mr. Ameed Amira, the head lab technician at the Chemistry Department laboratories, for their cooperation in making this job possible.

I also thank our collaborators in Canada, particularly Dr. Nashat Nassar Group for nanotechnology research, for their invaluable assistance in analysing our samples, which greatly contributed to this thesis.

Declaration

I, the undersigned, declare that I submitted the thesis entitled:

THERMO-OXIDATIVE DECOMPOSITION ANALYSIS OF PALM WASTES BY ISOCONVERSIONAL KINETICS AND AMMONIA FIBER EXPANSION

I declare that the work provided in this thesis, unless otherwise referenced, is the researcher's own work, and has not been submitted elsewhere for any other degree or qualification.

Student's Name: **Duha Abdalla Fathi Yousef**

Signature: Duha Yousef

Date: **20/02/2025**

List of Contents

List of Schemes

List of Figures

List of Tables

THERMO-OXIDATIVE DECOMPOSITION ANALYSIS OF PALM WASTES BY ISOCONVERSIONAL KINETICS AND AMMONIA FIBER EXPANSION

By
Duha Abdalla Fathi Yousef
Supervisors
Dr. Ismail Badran
Dr. Derar Smadi

Abstract

The study examines the thermal decomposition kinetics of raw and bleached palm leaves using thermogravimetric analysis, differential scanning calorimetry, and advanced isoconversional methods like Friedman (FR) and Kissinger-Akahira-Sunose (KAS). From the results obtained in thermogravimetric analysis, distinct degradation profiles in an oxidative atmosphere were observed: raw leaves from 215-565°C and bleached leaves from 200-490°C. Bleaching treatment reduces thermal stability due to lignin removal and hemicellulose, making the material suitable for bioenergy applications.

The kinetic analysis was conducted using the FR and KAS methods in order to determine the effect of the bleaching process. Bleaching decreased the activation energy which therefore increased the decomposition process. In contrast, the FR method gave a wider range of activation energies (300-440 kJ/mol), indicating more complicated reaction mechanisms in the bleached samples, while for the KAS method, the results of activation energy were more stable and lay within a narrow interval (140-190 kJ/mol), reflecting simpler reaction processes. Furthermore, differential scanning calorimetry studies showed that a high heating rate resulted in both a high decomposition temperature and total energy output. The energy release in bleached samples is higher (3411.33 a.u. at 25 °C/min) compared to raw samples (3107.67 a.u.), thus pointing to a significant role of chemical treatment on the decomposition efficiency.

The kinetic modelling showed that the values of the pre-exponential factor (A_α) and the activation entropy ($\Delta S^{\neq}$) for raw and bleached palm leaves are statistically different. Thus, at 25% conversion A_α values of raw palm leaves were higher by 1.4×10^{30} s^{-1} when compared to the bleached samples of 1.4×10^{26} s^{-1}. Raw palm leaves also exhibited a higher $\Delta S^{\neq}$ (318.5 J/mol·K) than bleached samples (241.9 J/mol·K), suggesting greater molecular disorder in the raw material. Thermodynamic parameters revealed that raw palm leaves required higher activation enthalpy ($\Delta H^{\neq}$ = 351.9 kJ/mol) than bleached samples ($\Delta H^{\neq}$ = 299.6 kJ/mol), indicating a more energy-intensive decomposition process.

Fourier transform infrared spectroscopy analysis confirmed structural changes, with the bleaching process reducing lignin and hemicellulose content, thereby simplifying the material's molecular structure.

Keywords: Palm leaves; Ammonia fiber expansion; Bleaching process; Thermogravimetric analysis; Differential Scanning Calorimetry; Isoconversional methods; Bioenergy production; Thermal stability; Kinetic parameters.

Chapter One

Introduction

1.1 Background

Global population growth, urbanization, and industrialization have led to increased production of complex solid waste, including sewage sludge, agricultural waste, solid waste from municipalities, food and household waste, garden trash, agro-industrial rubbish, and waste from animals. Thus, posing substantial environmental (1, 2).

Inadequate waste management methods, particularly in developed nations, such as open burning, pose significant environmental and health risks. Open burning is among the leading contributors to the amount of hazardous pollutants by emissions, including microparticles, responsible for 4.2 million premature deaths in the world and representing 6.7% of total deaths in 2016 (3). These particulates not only have adverse health effects, but they also contribute to climate change, absorbing sunlight and affecting cloud formation. Furthermore, waste incineration generates many toxic materials like polycyclic aromatic hydrocarbons (PAHs), nitrogen and sulfur oxides, polychlorinated dibenzo-p-dioxins (PCDDs), and metals that can have environmental and health consequences for many years (3).

Though one of the most popular methods of waste disposal, open dumping causes great harm to the environment. The model contaminates the land and releases poisonous and greenhouse gases that complete the murder of urban ground. In addition, it leads to the spread of waterborne diseases and negatively impacts air quality, increasing the problem of climate change (4). Among the main concerns of this method is the unsafe disposal of biodegradable organic waste, which is a major source of anthropogenic greenhouse gas emissions. The effects of this environmental degradation are not limited to the environment alone but also pose a significant threat to human health and well-being, along with economic losses (2).

The increase in green spaces along with urbanization has greatly increased the production of green waste, mainly comprising biomass such as grass, leaves, and pruning materials produced by gardens and parks (5-7). This kind of waste is normally related to garden waste, and fallen tree parts produced in great amount for aesthetic purposes in urban areas.

Green waste often consists of more than 90% of branches, leaves, and grass (8-10). With the increasing volume of this waste, proper management has become critical to ensuring urban sustainability.

Green chemistry seeks to create chemical practices that protect both humans and the environment from potential damage caused by chemical products and reduce the usage and production of hazardous compounds by promoting environmentally friendly alternatives (1, 11-13). Anaerobic digestion is one of the ways for converting organic waste into methane gas (1, 14, 15). Moreover, the circular economy idea is gaining popularity since it is founded on the concepts of reducing, reusing, recycling, and using the raw materials to create high-value products and minimizing waste (16, 17). This approach helps to increase product shelf life and encourages reuse after the effective time of usage has expired (1, 16, 18).

Agricultural waste, which made up approximately 11% of municipal solid waste in 2017, primarily consists of lignocellulosic materials that decompose slowly (19). The slow degradation of these materials leads to a range of problems, including aesthetic concerns, heightened fire risks, and methane emissions, which contribute to environmental degradation (19-21). Therefore, effective management of green waste is essential to urban sustainability initiatives (22). Advanced recycling technologies offer transformative potential by converting agricultural waste into high-value bio-based products and biofuels (23, 24). These innovations not only meet the growing demands of the bioeconomy but also facilitate the transition to a circular economy, aligning with the United Nations Sustainable Development Goals to promote environmental resilience and sustainable resource utilization (19, 25, 26).

The rising interest in green waste recycling systems seeks to reduce environmental impact, prevent resource depletion, reduce human health hazards, and preserve ecosystem equilibrium. Materials and energy recovery solutions, such as composting, this approach enhance soil fertility and crop productivity (2). Waste-to-energy incineration, anaerobic digestion, and pyrolysis and gasification are among the renewable energy conversion technologies under consideration (27). These methods provide indirect benefits to the environment, including lower emissions of greenhouse gases and preservation of land

(28). Economically, it saves land filling, transportation, imports, as well as chemical fertilizer manufacturing expenses while also creating rural job possibilities (2, 19).

Several studies have explored the potential of recycling agricultural waste (20, 29-32). For instance, Panuccio MR. *et al* (31)., investigated the possibility of transforming agricultural wastes into by-products to benefit the environment, soil fertility, and farm bio economy (31). Orange and olive waste emit different quantities of greenhouse gases, and using high sulfur fertilizers can help keep the environment clean (31). The economic benefits of converting garbage into fertilizer include the sale of new fertilizers, money saved from reduced chemical fertilizer manufacture, and lower land filling expenses (31, 33, 34).

In addition, Shokrollahi S. *et al*., studied the utilization of date palm leftovers as lignocelluloses for bioethanol and biomethane production in dry locations (32). The main palm residues were processed with phosphoric acid, resulting in a hemicellulose-rich liquor and cellulose-rich solid. Two situations were tested: bioethanol as well as biomethane generation from the processed liquor and solid. Untreated seeds and pre-treated leaves had the maximum ethanol output (32).

Palms, particularly in Palestine, play an integral role in the economy and culture (34). Known for their ability to thrive in diverse environments and its longevity of hundreds of years, the palm tree is extensively grown in regions such as Jericho, the Jordan Valley, and the Gaza Strip, notably in Deir al-Balah and Khan Yunis. Jericho, famously called the "city of palms," is celebrated for its vast plantations. By September 2021, Palestine hosted 571 palm plantations with over 311,000 palm trees (34).

Beyond their economic value for products like oil, dates, fiber, and decorative items. Palm waste remains largely underutilized (35). Each palm tree in Palestine generates approximately 15-20 kilograms of waste annually, amounting to an estimated 4,665 tons of palm waste (36). Unfortunately, much of this waste is either burned or left to decompose, contributing to environmental pollution, health risks, and increased flammability during storage. However, transforming palm waste into bio-related applications, such as absorbing harmful ions or generating energy, presents a promising solution to these challenges (37).

While fossil fuel dependence is further deteriorating the situation in terms of greenhouse gas emissions, air pollution, and climatic changes (38, 39), there is an increased urgency for renewable energy sources to take the fore (39). Biomass is obtained from organic material and constitutes a renewable and carbon-neutral energy carrier. The bio-energy uses chemical energy stored within organic substances due to photosynthesis and may then be released through the action of heat, converted into such fuels as biogas, biodiesel, or ethanol (39, 40). Biomass now provides around 10% of the total global supply of primary energy. Biomass is one of the major sources of energy in Palestine, especially in rural areas, accounting for about 9% of total consumption and mainly used for cooking and heating purposes (40). By using palm waste to produce biomass energy, Palestine can meet the environmental challenges while simultaneously solving the problem of sustainable energy. This approach reflects the ability of biological waste to support sustainable energy systems, thus reducing dependence on fossil fuels.

Bioenergy, which is obtained from biomass growth or waste/residues, is crucial for using bio-waste while lowering environmental effect. This technology offers practical options, such as employing renewable energy instead of fossil fuels in transportation, generating power for houses, and supporting agricultural operations (41). However, the energy sector in Palestine faces significant challenges, such as limited natural resources, unstable economic conditions, as well as dependence on imported fuel, which costs between $400 and $500 million per year (41). The move toward renewable energy minimizes these concerns by improving energy-related services, lowering harmful emissions, and improving economic resilience (42).

An example of renewable energy use in Palestine is the Palestine Technical University - Kadoorie project, which launched a pilot project based on solar panels in 2017, in addition to expanding the use of solar energy on the roofs of homes and commercial institutions, which indicates a growing interest in sustainable energy (42). These technologies play a key role in promoting energy independence and achieving long-term sustainable development in Palestine (42).

Moreover, An-Najah National University developed solar photovoltaic power systems under the Med-EcoSuRe project, which was sponsored by the European Union (13). The project focuses on renovating university facilities to be more energy efficient and integrating renewable energy sources. Currently, the institution has installed 220 kW of solar panels, with another 55 kW under development. The systems are grid-connected and installed on the rooftops of campus buildings such as the Faculty of Educational Sciences (62 kW) and the Faculty of Literature (105 kW). These projects aim to minimize CO_2 emissions, energy expenditures, and promote sustainable habits on campus (12, 13).

For this work, palm leaves wastes recycled to produce useful materials for Palestine's alternative energy source. Palm leaves wastes treated by Ammonia Fiber Expansion (AFEX), bleaching, and acidic hydrolysis. The thermal decomposition and oxidation of palm leaves wastes studied before and after treatment using a thermogravimetry analyzer and isoconversional analysis. To determine the kinetic (E_α) and the activation parameters ($\Delta H^{\neq}$, $\Delta G^{\neq}$, and $\Delta S^{\neq}$) for the oxidative decomposition of the palm leaves waste after and before treatments. In addition, their heat values determined using Differential Scanning Calorimetry. Their physical qualities also examined before and after processing by Fourier transform infrared spectroscopy and scanning electron microscopy.

1.2 Palm waste structure

Palm tree agro-industrial operations produce large leftovers, including empty fruit bunches, trunks, palm kernel shells, leaves, husks, as well as fibers. These wastes can harm the ecosystem and transfer pests to healthy palm trees (43). Among these, palm leaves waste, which accounts for a significant fraction, provides distinct potential and problems. This study will concentrate on the possible uses of palm leaves waste, especially its use in sustainable energy generation and other bio-related solutions, with the goal of transforming it from an environmental burden to a profitable resource.

1.2.1 Chemical structure

Palm has several applications, including papermaking, heavy metal absorption, soil fertilization, and energy production (37). Understanding a material's chemical composition is critical for its applicability for diverse uses, since it determines properties such as fungus attack, recycling, weather resistance, and fiber degradation (37). Palm is a plant having cellulose enclosed with hemicellulose as well as lignin, which form a lignocellulose structure (44). All these components are mostly connected by hydrogen bonds, although covalent bonds are also exist (39).

Najahi A and co-workers, revealed that date palm waste displayed lignin, hemicellulose, and cellulose concentrations of 28, 22 and 44 wt%, respectively. Ashes and extractives made up a residual fraction of the lignocellulosic feedstock (6 and 3 wt%) (45).

Cellulose, a fibrous organic polymer, plays a crucial role in various applications due to its unique structure and chemical properties. Composed of D-glucopyranose units linked by β-1,4-glycosidic bonds, cellulose forms a strong, crystalline structure that gives it remarkable resistance to water and degradation, as shown in the scheme 1. Its molecular arrangement allows it to serve as a sustainable, biodegradable material, making it a key resource in industries such as paper manufacturing, textiles, and packaging (46, 47).

The versatility of cellulose extends to its use in medical applications like wound dressing and tissue engineering (47). Its ability to be processed through various methods—such as mechanical grinding, steam explosion, and acid/alkali treatment—facilitates its extraction and refinement for a range of purposes. Additionally, cellulose's unique hydrogen bonding system, formed between hydroxyl groups, glycosidic bonds, and oxygen atoms, contributes to its solubility and crystallinity, impacting its overall performance in industrial processes (47).

Scheme 1

The structure of cellulose repeat unit (48)

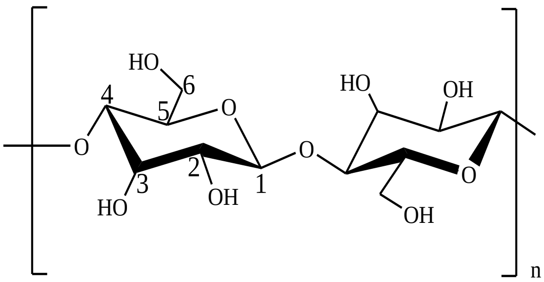

Hydrogen bonding have major effects on cellulose properties such crystallinity, solubility and hydroxyl group reactivity (47). These interactions are mediated by anhydroglucose units, D-glucopyranose ring oxygen atoms, and glycosidic bonds, which produce intramolecular and intermolecular hydrogen bonds that contribute to the rigidity and stiffness of cellulose (47).

Cellulose molecules include intramolecular bonds between hydrogen and oxygen atoms within the molecule itself, which make cellulose an extremely rigid material and cause particularly viscous liquids to form crystals (47). While hydrogen bonds between distinct cellulose molecules, known as intermolecular bonds, are weak bonds, they operate to produce layers of cellulose when combined with hydrophobic interactions, further affecting its physical characteristics (47).

Hemicellulose, an organic polysaccharide, is a major renewable component of lignocellulosic biomass, accounting for 60 billion tons globally each year (49). Its exceptional qualities make it helpful in a variety of materials and fine compounds used in food, medicine, and energy storage. However, typical kraft pulping destroys hemicellulose, resulting in inefficient usage. Improved cellulose accessibility requires efficient removal (49).

Hemicellulose, a form of polysaccharide, accounts for 15%–35% of plant dry mass, the kind of hemicellulose is determined by the plant's species, cell type, location, and stage of development (49). It composed of pentoses, alternating mannose and glucose units, or galactose units. It consists of 50-3000 sugar units, unlike cellulose, which has 7000-15,000 molecules of glucose per polymer (50), is shown in the scheme 2.

Scheme 2

A representative structure of Hemicellulose (51)

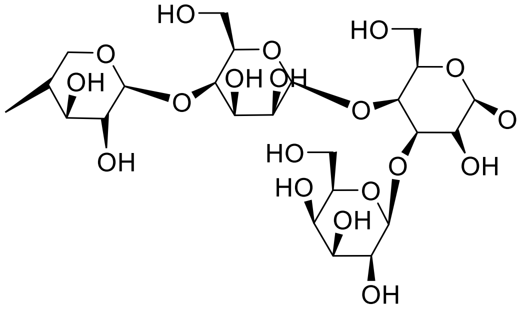

Lignocellulosic biomass's hemicellulose is transformed into fuel-grade oligosaccharides (49). Ethanol production requires efficient hemicellulose removal. An effective biorefinery should pre-extract and isolate hemicellulose to enhance resource efficiency and biomass utilization. The complicated cell wall structure of lignocellulosic biomass makes it resistant to chemical and enzymatic treatments, necessitating more investigation for effective separation (49).

Lignin, a three-dimensional amorphous aromatic polymer, is the second-most common biopolymer after cellulose, accounting for over 30% of organic carbon in the environment. This renewable aromatic polymer is composed of phenylpropanoid units derived from three cinnamyl alcohols—p-coumaryl, coniferyl, and sinapyl (52, 53). As shown in the scheme 3.

Scheme 3

The structure of Lignin (54)

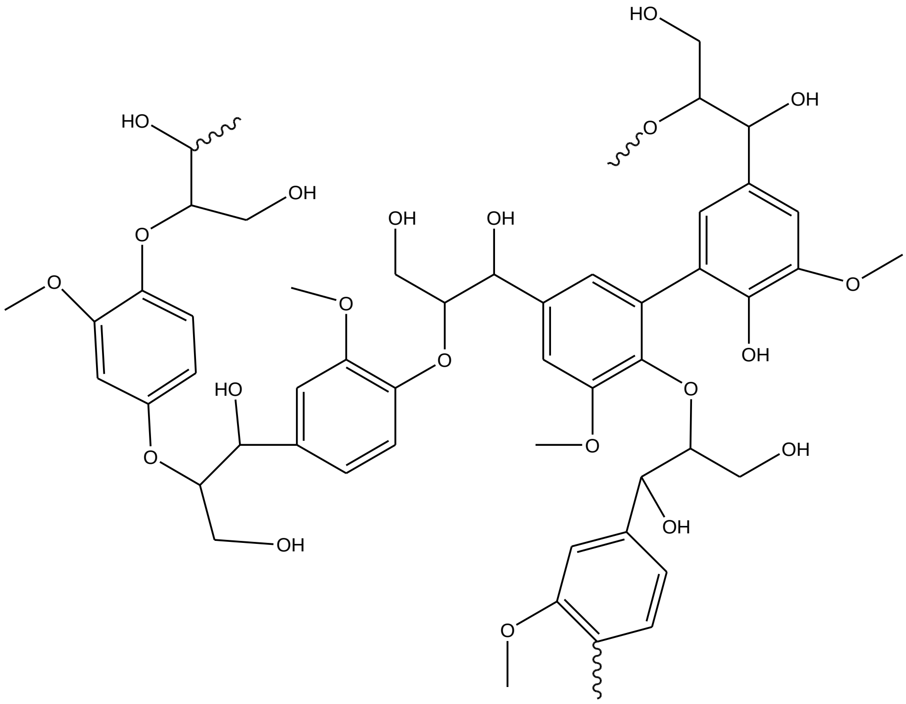

Lignin plays a critical role in plant cell walls by providing strength, rigidity, and protection against microbial infections, in addition to acting as a physical barrier to diseases and insects (55). Known as the "glue" of the plant cell wall, it serves as a binding agent in the cellulose/hemicellulose matrix (53).

In various industries, lignin is utilized extensively, particularly in the pulp and paper sectors, where it contributes to the production of 50-60 million tons per year (52). It is also used in lubricants, dispersion agents, and as a replacement for inorganic fillers in polymeric materials, enhancing thermoplasticity, biodegradability, and mechanical properties. Lignin's resistance to oxidation, high temperatures, and its antifungal, antioxidant, and antibacterial properties make it valuable for producing biomaterials, including composite hydrogels (56). Moreover, recent research in biorefineries has focused on lignin-based materials such as hydrogels, microparticles, granules, microcapsules, nanocapsules, and nanoparticles (52).

Palm waste's lignocellulose composition has led to interest in converting it into a useful and economically feasible material for future applications (57).

1.2.2 Physical properties

Palm tree is about 23-meter-hight tree with a top layer of pointed leaves that are around 5 meters tall (58). Its stem is clearly characterized with clipped stubs of old leaf bases, and male and female flowers grow on distinct plants. Female flowers under cultivation are pollinated artificially. Dates are one-seeded, rectangular fruits that vary in form, size, color, quality, and consistency. A single bunch weighing eight kilograms or more can contain more than 1,000 dates (58). Palm plants are reproduced via seeds or suckers. They being bearing fruit in 4 to 5 years and reach full bearing in 10 to 15 years, producing 40 to 80 kg or more apiece. Palms may endure for up to 150 years, although their fruit output decreases (58).

1.3 Palm waste treatment

Various studies have explored the treatment of palm tree wastes and their applications in addressing critical issues (59-61). For instance, Aloud, S.S., *et al*. studied activated carbon generated from date palm stones as an adsorbent to extract the hazardous dye remazol brilliant blue R. The production of activated carbon from date palm stones required chemical treatment with NaOH and KOH, resulting in significant Brunauer-Emmett-Teller (BET) surface area, Langmuir surface area, average pore diameter, and overall pore volume. The adsorption process was most effective under acidic conditions, with an absorption capacity of 98.33 mg/g for Remazol Brilliant Blue R (59).

Also, Mahdi Z. *et al*., investigated that date seed-derived biochars effectively remove lead ions from aqueous solutions (60). The biochar produced at 550°C for 3 hours performed the best for lead ion elimination. Under ideal conditions, this biochar showed a high adsorption capability, making it a useful material for heavy metal removal. This study emphasizes the possibility of employing agricultural waste, such as date seeds, to generate biochars that can solve environmental pollution challenges, notably in water treatment operations (60).

In another work, Mehrez and colleague investigated the effect of ionic and alkali liquid pre-treatment on biochemical methane potential of date palm waste (61). The study reported that processing palm and fruit bunches using ionic liquids resulted in high Biochemical Methane Potential (BMP) efficiency of substrate during conversion. While pre-treatment with alkalis showed excellent effectiveness when applied to palm waste of all sorts, and this study highlights the relevance of pre-treatment in enhancing the efficiency of anaerobic digestion to create methane from date palm trash (61).

1.4 Biomass pyrolysis

Pyrolysis is a promising bioenergy method that converts biomass into synthesis gas, bio-oil and coal using heat (62, 63). These by-products have great energy potential and can be used for energy recovery, being considered renewable energy source or a sustainable alternative to conventional fuels, activated carbon and Fertilizers. Also pyrolysis supports advanced carbon capture and sequestration, and this helps to mitigate greenhouse gas emissions (64). The pyrolysis process is basically a series of reactions that occur when heating organic substances in the absence of oxygen. These reactions include dehydration, depolymerization, fragmentation, rearrangement, re-polymerization, condensation, carbonization (63, 65, 66). Through reading several studies that have dealt with this topic, I noticed that this mechanism is widely used with various types of biomass, highlighting its importance in generating clean energy and reducing waste by converting it into value-added materials (63).

Pyrolysis is the most researched thermo chemical method, producing gas, liquid, and solid biofuels by degrading biomass components in an oxygen-free environment under particular heating conditions (39). It is a simple and inexpensive method for turning organic resources into energy-rich compounds. Biomass materials, particularly lignocellulosic or polluted biomass, can be converted into bio-oil, biochar, and pyrolytic gases. Several strategies can be implemented before, during, and after pyrolysis (67). Physical procedures such as grinding, heat treatment, and chemical treatment can eliminate moisture and impurities, hence raising H/C ratios also increasing energy content and fuel characteristics. Additionally, the use of advanced catalysts can further improve the quality of bio-oil produced during pyrolysis (39).

However, conventional pyrolysis processes that burns biomass completely, turning it mostly into CO_2 and H_2O. This is a big disadvantage (68). While pyrolysis can produce significant heat, it does so at the cost of reducing the chemical value of the biomass since the energy content is generally absorbed during burning. This limitation has prompted the development of new ways for increasing both heat production and the synthesis of valuable chemicals.

In this study, biomass recovered from palm leaves wastes was processed by ammonia fiber expansion pretreatment, which helped to improve biomass digestion and reactivity, as well as resulting in more effective extraction of high-value products. Then, the palm leaves bleached to produce nanocellulose. It removed lignin and hemicellulose, resulting in pure cellulose with improved characteristics.

1.5 Ammonia Fiber Expansion (AFEX)

The AFEX pre-treatment is a novel alkaline process that includes the physical and chemical treatments to improve and alter the lignocellulosic material structure, which enables ammonia recovery and its reutilization. It is simpler than other pre-treatment procedures and improves enzymatic digestibility (69). Concentrated ammonia is employed for breaking down the resistance of plant biomass and increases its reactivity for pyrolysis processes. It works well with maize stover, and rice straw, but its efficiency with palm plantation leftovers is uncertain (70). This process occurs in a specialized reactor with temperature and pressure control, in which biomass is mixed with liquid ammonia in a ratio of 1:1 or 1:2 at 60-120 °C and 2 MPa pressure for 10-60 minutes.

The combination is heated to the necessary temperature, then pressure is released. This causes the ammonia to evaporate, resulting in a drop in the system's temperature (39). AFEX pre-treatment process involves breaking down the crystalline structure of cellulose, partially depolymerizing hemicellulose, removing acetyl groups, and disrupting lignin-carbohydrate complexes through lignin C-O-C bond cleavage (39). This process increases the accessible surface area and enhances the wettability of the treated biomass. As a result, the biomass undergoes significant structural changes, potentially improving its thermal stability, bulk density, particle density, and the durability of pellets (39, 69). These improvements demonstrate promising economic advantages when compared to alternative pre-treatment technologies (39, 69). Scheme 4 shows a schematic representation of the ammonia fibre expansion reactor.

Scheme 4

A schematic of AFEX reactor setup and heating system (69)

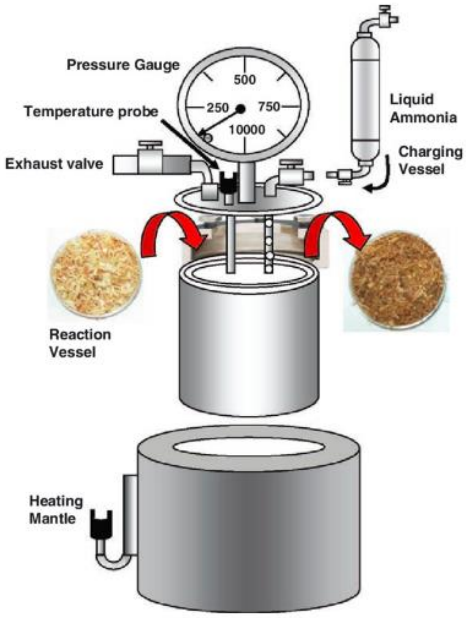

There are many studies that have been interested in treatment of AFEX (71-73). For instance, Qiao X. *et al*., investigated the use of hydrogen peroxide soaking before AFEX (H-AFEX) as a pre-treatment method. Their research demonstrated its effectiveness in reducing biomass resistance and improving enzymatic accessibility (71). They analyzed ball-milled wood lignins and found that H-AFEX-treated lignins exhibited increased oxygen and nitrogen levels, decreased carbon and hydrogen content, and significantly reduced molecular weight. These findings suggest H-AFEX could be a promising approach for advancing biomass bioconversion techniques (71).

In another study, Hoover AN. *et al*., examined the impact of pelleting process variables on the physical properties and sugar yields of AFEX-treated corn stover (72). Their study showed that pelletized AFEX-treated corn stover had enhanced bulk density and durability compared to untreated or solely AFEX-treated pellets. Interestingly, enzymatic hydrolysis sugar yields remained consistent regardless of die speed, while pellets preheated or with larger grind sizes produced equal or lower sugar yields (72).

Also, Passetti RA. and co-worker, studied and investigated the effects of AFEX treatment on rice straw degradability, growth performance, microbial colonization, as well as acetamide levels in ewe lambs (73). Their results showed that AFEX treatment transformed rice straw into a more digestible fodder and altered the microbial biofilm composition, aligning it closer to that of alfalfa. However, lambs consuming a pelleted diet with 25% AFEX-treated rice straw did not gain weight, likely due to reduced feed intake and lower feed efficiency (73).

1.6 Nanocellulose

Cellulose is an important biopolymer and sustainable raw resource, and nanocelluloses are cellulosic polymers having at least single dimension in the range of the nanoscale (74). These nanocelluloses merge the properties of cellulose with those of nanoparticles, enabling novel biological, environmental, and technological applications. They also show the growing integration of biological and material engineering (74).

Nanocellulose is a flexible, low-cost bio-based material that is both biodegradable and non-hazardous with potential uses in high-performance composites. Its low energy consumption and value make it an excellent waste treatment option (75). There are various approaches for separating and purifying nanocellulose, and combining them may impact the morphology of the fibers. This low-cost, multifunctional material has attracted industrial attention (75). It is made up of cellulosic extracts with a diameter of less than 100 nm, which include cellulose, the primary component of lignocellulosic fibers (76).

Nanocellulose is classified into three types: bacterial nanocellulose, cellulose nanofibrils, as well as cellulose nanocrystals. Bacterial nanocellulose is created biotechnologically by bacteria, cellulose nanofibrils are mechanically delaminated by plant-based cellulose, and cellulose nanocrystals are separated via chemical hydrolysis or oxidation. They are sustainable, plentiful and inexpensive materials (74, 76). They have appealing qualities such as wide surface area, outstanding stiffness, excellent strength, high elastic modulus, low density, dimensional stability, as well as minimal thermal expansion (77, 78). Due to their unique physicochemical properties, they are considered a valuable category of advanced materials for the future. which make them helpful in polymer nanocomposites, textiles, catalysis, tissue engineering, green nanocomposite materials, packaging of food, and delivery of medicines (77, 78).

The previously mentioned categories of nanocellulose may be created utilizing a variety of techniques and cellulosic materials. The shape, size, and various attributes of each class depend on the cellulose source, the conditions used for isolation and processing, and any treatments applied before or after these processes. The ability to generate nanocellulose with a variety of properties is interesting because it can encourage the discovery of hitherto untapped biomass. The 3D hierarchical nanostructure and nanoscale physicochemical properties open up new opportunities across various applications. The nanocellulose market is projected to grow to $783 million by 2025 (77).

Nanocellulose extraction from plant fiber sources has been extensively researched worldwide (78). Mechanical procedures, such as extreme pressure homogenization, cryocrushing, and ultrasonication, along with chemical treatments like TEMPO-mediated oxidation, are commonly employed. TEMPO (2,2,6,6-Tetramethylpiperidine-1-oxyl) is a stable free radical compound used to oxidize cellulose fibers. The most generally used approach is TEMPO-mediated oxidation, which involves oxidizing cellulose fibers with $NaClO$ in an aqueous solution to produce cellulose nanofibrils with a large aspect ratio (78).

There are many studies that have been interested to produce nanocellulose. For instance, Nor Fazelin MZ. *et al*., have studied Pomelo peel, a high-fiber waste product, has the potential to produce useful substances (79). A research extracted and analyzed cellulose also nanocellulose from pomelo albedo. Cellulose was manufactured by alkali treatment and bleaching, whereas nanocellulose was created via sulfuric acid hydrolysis. The physicochemical and structural characteristics were investigated utilizing proximate analysis, Fourier Transform Infrared Spectroscopy (FTIR), and X-ray Diffraction (XRD). The study indicated that pomelo albedo can provide natural cellulose and nanocellulose materials for usage in culinary components (79).

In another study, Hop TT. And coworker, focused on the production of nanocellulose from bleached wood pulps utilizing a TEMPO-mediated oxidation process with sodium hypochlorite as an oxidant (80). The study looks at how pH levels, oxidant concentration, and ultrasonic times affect the oxidation of cellulose molecules. Nanocellulose's structure as well as characteristics were studied using FTIR, Scanning Electron Microscope (SEM), XRD, and phase-contrast microphotographs. The best conditions for reaction were 10 mmol/g NaClO, pH 10, and an oxidation duration of 253 minutes (80).

Also, Henao Rodríguez JE. *et al.,* studied and extracted the cellulose microribbons of coffee parchment using alkaline hydrolysis, bleaching, as well as acid hydrolysis techniques (46). They found that both the concentrations of chemical precursors and reaction durations influenced mass losses. The hydrolysed and bleached parchment was characterized using techniques such as SEM, Thermogravimetric analysis (TGA), XRD, and FTIR (46). The results revealed that hemicellulose was the primary fraction produced, whereas lignin was liberated following alkaline hydrolysis. The study discovered that the concentration of chemical precursors had a substantial impact on cellulose quality, with best extraction conditions being 5% HNO_3 after 2 hours, 3% NaOH after 1 hour, and a 1:1 ratio of NaClO:CH_3COOH after 45 minutes (46).

Additionally, Hamed O *et al.,* studied the production of magnetic nanocellulose from olive industry solid waste (81). The purpose of this study is to determine the efficiency of magnetic cellulose nanocrystalline in extracting methylene blue from polluted water. Thermodynamic studies revealed that magnetic cellulose nanocrystalline absorbs methylene blue spontaneously at various temperatures. It concentrated on enhancing the magnetic nanocellulose characteristics, which increased its efficacy in removing contaminants from water. This strategy was intended to provide a long-term solution for wastewater treatment by employing waste products from the olive industry (81).

1.7 Thermogravimetric analysis

TGA is a technique for measuring mass changes in a material as temperature varies, providing precise information on thermal stability, reactivity, reaction mechanisms, decomposition kinetics, content determination, and compositional analysis (82, 83). It is commonly utilized in kinetic investigations that include chemical and material devolatilization. TGA is often employed to determine the moisture and volatile levels in materials such as coal, biomass, pharmaceutical waste, and sewage waste (84). TGA analysis is typically performed using two methods: isothermal and non-isothermal. Isothermal methods are less commonly utilized due to their lower accuracy and modest weight loss, whereas non-isothermal methods are more dependable and efficient in time. TGA data may be analyzed using both model-fitting and model-free (isoconversional) methods. Isoconversional methods estimate complicated chemical processes with an accuracy of less than 1% (85).

TGA can additionally identify residual solvents and water content in materials. It helps to identify organic compounds and inorganic materials such as metals, polymers, plastics, ceramics, glasses, and composites. Samples can be evaluated as powder or in minutely pieces (48, 86, 87).

A sample is thermally treated by measuring temperature, time, and mass simultaneously in a controlled dynamic environment. A microbalance is used to quantify weight loss as a result of thermal treatment. The sample is placed in a specifically built container, and the temperature is adjusted using proprietary software. The sample pan is attached to a sample holder and is usually constructed of alumina, platinum, or aluminum (88, 89). Scheme 5 shows the diagram of the TGA device.

Scheme 5

The diagram of a typical TGA system (90)

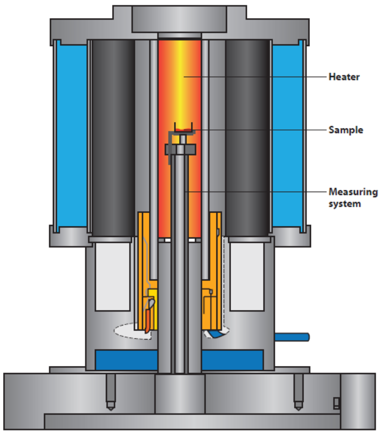

TGA parts are the thermos balance is the core of a TGA unit, comprising many sub-units such as an electronic microbalance, sample container, furnace, temperature programmer, and recorder (91). Commercial TGAs may reach above 1000°C, have a balancing sensitivity of 0.1 μg, and have a variable heat-up rate of 0.1-200°C/min under air or gas (92).

The TGA curve depicts weight change based on temperature or time during an individual stage of decomposition. The temperatures at which decomposition begins and ends are denoted by "T_i" and "T_f," respectively. The values of T_i and T_f are determined by the sample's thermal stability (91).

TGA may be used to explore both physical and chemical events, physical events such as vaporization, desorption, absorption, and sublimation. And chemical events such as the dehydration, oxidation, combustion, and decomposition (82).

TGA is a straightforward method for calculating the kinetic characteristics of organic materials or thermochemical processes (85). It employs models like one step reactions, parallel dual reactions, three-pseudo components, as well as the distributed activation energy approach to determine combustion and pyrolysis processes. The kinetic behavior of lignocellulosic biomass is studied to better understand pyrolysis reactions, anticipate correct data, and improve thermal degradation processes. TGA also helps to build effective thermochemical processes (85).

An example of TGA utilization in cellulose analysis is the pyrolysis of cattle dung, where TGA tests are conducted at multiple heating rates and isoconversional techniques to quantify activation energy (93). The thermodynamic properties, including the pre-exponential factor, enthalpy, free Gibbs energy, and entropy variations, are investigated. The findings identify a three-stage reaction with increasing conversion rates: extractives and hemicellulose, followed by cellulose and lignin, and finally lignin along with mineral components. The decomposition mechanisms of every component interact, exposing the complex process of cattle dung pyrolysis (93).

1.8 Isoconversional analysis

Isoconversional techniques study reaction kinetics and determine characteristics such as activation energy (E_α) without analysing the reaction model (94). They compute activation energy at various heating rates while holding another factors constant. According to the concept, the rate of conversion is evaluated at specific temperature or heating rate intervals, typically four to five. Techniques such as Kissinger-Akahira-Sunose (KAS) and Friedman (FR) are applied to develop kinetic models and determine associated parameters. To calculate activation energy for distinct decomposition mechanism phases, data sets were analyzed using the KAS and FR isoconversional techniques (94).

The extent of conversion can be easily calculated by measuring any physical property that varies with the reaction's progress. For this work, if the reaction progress is tracked through the change in mass using TGA, the extent of conversion (α) is calculated by taking the ratio of the current mass loss (Δm) to the total mass loss (Δm_{tot}) observed throughout the process (95).

Where α is given by:

$$\alpha = \frac{m_0 - m}{m_0 - m_f} = \frac{\Delta m}{\Delta m_{tot}} \quad [1]$$

Here, m_0 represents the initial mass of the sample, m_f signifies the final mass, and m denotes the mass of the sample at a specific time during the process.

The reaction order may be used to describe homogeneous reactions, as follows (95):

$$f(\alpha) = (1 - \alpha)^n \quad [2]$$

Using the temperature dependency of the isoconversional rate, we may estimate the activation energy values (E_α) without identifying or making assumptions about the reaction model (95). This is to identify the parameters of the primary two equations that will tie into the method, which are [3] and [4] below (95):

$$\frac{d\alpha}{dt} = k(T)\, f(\alpha) \quad [3]$$

Here, t represents time, T denotes temperature, and k(T) corresponds to the temperature-dependent rate constant, f(α) is a function that represents the reaction mechanism (95). And the rate constant is related to temperature through the Arrhenius equation.

$$k(T) = A_\alpha \exp\left(-\frac{E_\alpha}{RT}\right) \quad [4]$$

Here, A_α is the pre-exponential factor, and R is the universal gas constant (95).

The isoconversional method uses a unique rate equation for each degree of conversion and a limited temperature range, ΔT, linked to that specific conversion. By utilizing distinct heating rates, β_1 and β_2, the approach enables to determine various rates for the same conversion, as shown in the equation below (95):

$$\frac{d\alpha}{dt} = \beta \left(\frac{d\alpha}{dT}\right) \quad [5]$$

Therefore, if the goal is to determine the effective activation energy, enter equation [4] into equation [5], this generates the following equation [6] (95):

$$\frac{d\alpha}{dT} = \left(\frac{A_\alpha}{\beta}\right) \exp\left(-\frac{E_\alpha}{RT}\right) f(\alpha) \quad [6]$$

After getting the temperature dependency of the isoconversional rate using a series of temperature programs, and applying the previous equations to the data, it can be parameterized by the differential isoconversional equation from FR (94-96):

$$ln\left(\frac{d\alpha}{dt}\right)_{\alpha,i} = ln[A_\alpha f(\alpha)] - \frac{E_\alpha}{RT_{\alpha,i}} \quad [7]$$

Here, $\frac{d\alpha}{dt}$ represents the reaction rate, T is the absolute temperature in Kelvin, A_α is the pre-exponential factor, E_α is the activation energy, R is the universal gas constant (8.314 J/mol·K), and f(α) is the reaction model function. i denotes the specific temperature program setting corresponding to each solution of the equation.

Another common equation that is used for the determination of E_α is the KAS equation (94-96):

$$ln\left(\frac{\beta_i}{T^2_{\alpha,i}}\right) = const \; - \frac{E_\alpha}{RT_{\alpha,i}} \quad [8]$$

This method is useful for determining the E_α. To calculate it, plot ln (ß $\frac{d\alpha}{dt}$) against 1/T(K) for all heating rates using the FR method, and ln ($\frac{ß}{T^2}$) against 1/T(K) for the KAS method. The slope of the best-fit line can then be determined, as will be discussed in Chapter 2.

For instance, a study was conducted utilizing TGA to explore the thermal behavior and oxidative decomposition of the antidiabetic drug glimepiride under both nitrogen (N_2) and oxygen (O_2) environments(94). KAS and FR's isoconversional techniques were utilized to determine effective activation and bond dissociation energies. Bond dissociation energies were estimated using density functional calculations. The research analyzed the pre-exponential factor alongside the kinetic triplet parameters ($\Delta H^{\neq}$, $\Delta S^{\neq}$, and $\Delta G^{\neq}$) to evaluate the upgrading processes of solid wastewater (94).

In another study, Nie N *et al.*, studied the kinetic mechanism of switchgrass pyrolysis utilizing isoconversional kinetic analysis and a master plots method (97). The pyrolysis kinetics were investigated using TGA at various temperatures. The results revealed a considerable conversion dependency of activation energies, indicating a complicated mechanism including overlapping decomposition processes. The research also identified a kinetic compensation relationship between the frequency factor and activation energy (97).

1.8.1 Differential Scanning Calorimetry (DSC)

DSC is a thermoanalytical method that detects heat flow or temperature differential between test sample and reference at a constant rate of temperature increase or decrease (92). It provides quantitative and qualitative information regarding physical and chemical changes that occur during endothermic or exothermic processes, as well as changes in the material's heat capacity. In a temperature range from -60 °C to over 1500 °C (92).

It measures the temperature-dependent change in a material's heat capacity (C_p), also detecting transitions including melting, glass transitions, and phase changes (86). Its applications are very diverse including the fields of medical, printing, cooking, agriculture, plastics, manufacturing, paper and electronics. A thermogram shows temperature on one axis and heat flow on the other, offering extensive insights into thermal characteristics (86).

Also it is an effective technique for identifying soil organic matter, clay minerals, and contaminants (98). DSC has also been used to investigate microplastics, which are extensively dispersed in many settings. Branching, impurities, additives, and sample size can all have an effect on microplastic polymer phase transition temps. DSC is often related to other thermal techniques such as TGA, differential thermal analysis, and microcalorimetry (98).

DSC has been extensively used in the biopharmaceutical industry for the characterization and development of manufacturable medicinal products, especially therapeutic proteins in dilute liquids and solid forms (99). DSC measurements of solutions and solids require instrument configurations that provide high sensitivity for solution analysis but generally use standard instrument setups for solid-phase measurements. Such flexibility in instrumentation allows DSC to be effectively used for a wide range of applications in drug development and formulation (99).

DSC measures the extra heat released or absorbed by a sample during temperature changes by analysing the temperature difference between the sample and a reference material. This is represented as endothermic or exothermic peaks on the DSC curve (100). A standard DSC operates isothermally or with a constant temperature change within a controlled atmosphere. The heat flow, or enthalpy change, is then displayed versus time. Both endothermic and exothermic activities produce an enthalpy peak, providing insight into the thermal behavior of the material (92).

1.9 Aims of the study

The primary purpose of this study is to investigate the process of palm leaves decomposition before and after processing using AFEX and bleaching treatment, with an emphasis on thermal kinetics utilizing the isoconversional method. In this study, we seek to understand the changes that occur when palm leaves are heated, the products resulting from thermal decomposition, as well as the possibility of producing carbon-free fuel through these processes. The cellulose used in this research was also extracted from palm leaves that were previously processed through a multi-step procedure (101). Then, the isolated cellulose is converted into nanocellulose fibers using a combination of bleaching and acid hydrolysis, which is the second main objective of the study.

Also, it aims to analyze untreated raw palm leaves and cellulose nanofibers in terms of chemical and physical structure using SEM, FTIR, DSC, and TGA. These techniques are used to understand the changes that occurring in raw and bleached palm leaves, as well as to assess the effectiveness and efficiency of bleaching and decomposition processes, and explain how these treatments influence the diverse qualities of leaves and fibers by carefully analysing these materials.

1.10 Novelty of the study

This study aims to develop a new and environmentally friendly method for converting palm leaves into high-value nanocellulose fibers. Unlike traditional methods that rely on environmentally harmful procedures, it relied on AFEX technology followed by bleaching and acid decomposition processes to achieve more efficient conversion while reducing the environmental impact and enhance the efficiency of nanofiber extraction and refining.

Unlike previous studies, which focused primarily on structural and chemical changes using techniques such as SEM, FTIR, and XRD, this work used TGA in conjunction with isoconversional methods to analyze the decomposition dynamics and thermal stability of palm leaves before and after treatment. Our advanced study measured activation energy and other parameters ($\Delta H^{\neq}$, $\Delta G^{\neq}$, and $\Delta S^{\neq}$) during the decomposition process. Through this study, we want to provide a novel method for converting agricultural waste into high-performance materials, thus contributing to the development of sustainable materials and new uses in the field of renewable energy.

Chapter Two

Materials and experimental methods

This work considers the complete investigation of kinetic behavior through the use of isoconversional methods in order to determine the kinetic and activation parameters of palm leaves waste and its thermo-oxidative decomposition after bleaching and acid hydrolysis treatment.

2.1 AFEX pre-treatment

Raw palm leaves were obtained from Jiftlik farms near Jericho, it was dried at An-Najah National University laboratory away from the sun. Using a blender, the raw palm leaves were crushed for a particle size range of approximately 1-10 mm to enhance the surface area available for ammonia penetration. The raw palm leaves were placed in a high-pressure reactor (1 L stainless steel). The biomass-to-ammonia ratio was maintained at approximately 1:3 (w/w). A balance was used to weigh 15.02 grams (dry weight) of raw palm leaves powder. To prepare the reactor mixture, 100 mL of distilled water was mixed with palm leaves powder to achieve the desired moisture content. Then, 200 mL of ammonium hydroxide was added to the reactor vessel. The reactor's lid was securely fastened, the entire reactor assembly was then placed in a Buchiglasuster BMD 300 heating mantle to achieve the desired reaction temperature (102). Figure 2.1 illustrates the ammonia fiber expansion reactor (Buchiglasuster).

The reactor temperature was brought up to about 80-90°C to increase the solubility of ammonia and, therefore, the effectiveness of the treatment. To avoid overheating, the apparatus was immersed in bath water at constant temperature. Pressure inside the reactor needed to maintain liquid ammonia during the treatment was 8 ± 1 bar. These conditions were sustained for two hours.

After the treatment, the reactor was gradually cooled to minimize thermal stress on the palm leaves (biomass). Once the cooling process was complete, the reactor was opened suddenly to relieve pressure (103). This quick decompression is required to allow the biomass fibers to expand, increase their surface area, and become more reactive for following treatments such as enzymatic or chemical procedures. The quick release of pressure creates an explosive discharge, allowing it to break down the lignin-carbohydrate complexes, a critical step in enhancing biofuel production efficiency (103). Following processing, the palm leaves were delicately washed with vast volumes of water to ensure that any leftover ammonia was removed and the material was completely purified. After that, the cleaned palm leaves were placed on trays and dried in an oven at a low temperature of 40°C to 60 °C until they appeared dry.

Figure 2.1

AFEX reactor setup and heating system, using a Buchiglasuster BMD 300 heating mantle instrument

2.2 Cellulose extraction

The AFEX-treated palm leaves were collected and finely powdered to a size of 1–5 mm. After that, the material was dried in an oven at 60 °C until its mass was stable. for the bleaching process, 50 g of AFEX-treated palm leaves were used, 1.2 L of 1% sodium hypochlorite solution, 200 mL of distilled water, and 1 g of sodium hydroxide, with a pH adjustment to 10-11 to optimize bleaching effectiveness (101).

The AFEX-treated palm leaves were collected and finely powdered to a size of approximately 1–5 mm. After that, the material was dried in an oven at 60 °C until its mass was stable. for the bleaching process, 50 g of AFEX-treated palm leaves were used, 1.2 liters of 1% sodium hypochlorite solution, 200 mL of distilled water, and 1 g of sodium hydroxide, with a pH adjustment to 10-11 to optimize bleaching effectiveness (106).

The experiment was carried out in a 2 L beaker, with mechanical stirring to ensure complete reactivity. The bleaching treatment required 48 hours at 25 °C. The experiment was monitored until the color convert to the white which indicated the effectiveness of lignin removal (101). Then the solid cellulose obtained from the bleaching solution was extracted using a filtration device. The solid cellulose obtained from the bleaching solution was extracted using a filtration device. The product was thoroughly rinsed using distilled water to remove any residual bleaching chemicals, continuing until the effluent became neutral (pH ~7). Washing and filtration were performed three times to ensure thorough purification.

The filtered product was then transferred to a 1 L beaker containing 10 mL of 0.3% hydrogen peroxide. The mixture was stirred mechanically at room temperature for an hour to ensure that pure cellulose was obtained (101). After that, the second filtration process was carried out in order to extract the treated cellulose from the H_2O_2 solution, which improved the quality of the final material. Then the cellulose was deeply cleaned with water to remove any leftover chemicals and obtain a high level of purity. Finally, the cellulose was dried in an oven set at 60-80 °C. To assure the completed product's quality, it was then put in a desiccator that prevented any moisture from being reabsorbed.

2.3 Nanocellulose extraction

The palm leaves were bleached and then subjected to acid hydrolysis. In this procedure, the process was carried out by adding 500 mL of 1 M hydrochloric acid to a 1-liter beaker containing 2.5 g of bleached palm leaves, and then the mixture was stirred mechanically. This treatment was conducted for two hours at 25 °C (81). The resulting nanocellulose was thoroughly washed with distilled water 3-5 times to remove any leftover acid. Finally, the washed nanocellulose was dried in an oven set to 60 °C until a consistent weight was achieved.

2.4 Experimental thermochemical analysis, using isoconversional methods

The isoconversional method, also known as the model-free approach determines activation energy without requiring a predefined reaction model, as mentioned previously in Chapter 1, section 8.

The principles of the Isoconversional Method:

1. Constant conversion analysis: The method analyzes the reaction rate at specific conversion levels (α), allowing for a more flexible evaluation of kinetic data.
2. Kinetic model: The kinetic equation, as described in Chapter 1 (Equation 3), specifies the reaction rate in relation to temperature and conversion.
3. Arrhenius Equation: Introduced in Chapter 1 (Equation 4), expresses the temperature dependence of the rate constant in chemical reactions. It demonstrates how reaction rates increase with rising temperature. The equation relates the rate constant k to the temperature T, activation energy E_{α}, and a pre-exponential factor (95).
4. Activation Energy Determination: E_{α} can be derived using the following relationship (95):

$$E_{\alpha} = -R \frac{d\,(\ln k)}{d\,(1/T)} \qquad [9]$$

Arrhenius charts, derived from the Arrhenius equation, graphically illustrate the relationship between temperature and the rate constant.

The Arrhenius plot is based on a linear relationship; plotting ln(k) against 1/T usually yields a straight line. The slope of this is proportional to the activation energy (E_{α}) and the gas constant (R) with an intercept of ln(A). To correctly acquire the slope and intercept, a linear regression line is fitted, from which the actual values of E_{α} and A may be obtained more precisely. This approach is critical for understanding the temperature dependency of reaction rates as described by chemical kinetics. Linear regression is a statistical approach that models a relationship between two continuous variables; hence, it is useful in determining the significance of the kinetic parameters from Arrhenius plots (104).

The basis of linear regression:

1. The model for a straight line is provided by following equation (104):

$$y = mx + b \tag{10}$$

Here y is the variable of dependent (such as, ln(k)) , x is an independent variable, such as $1/T$, m = slope (which is $-\frac{E_\alpha}{R}$), and b = y-intercept (related to ln(A)).

2. Least squares approach: To choose the best-fitting line between the data points, the method minimizes the sum of squared residuals.
3. Fit Quality: The coefficient of determination (R^2) evaluates the model's fit to the data, with values nearer to 1 signifying better fit.

A statistical indicator of a regression model's capacity to describe the variability of the dependent variable is called R^2. A score of 1 indicates a faultless explanation; it goes from 0 to 1. When predictions closely match observed values, the model is better fitted to the data, as shown by a higher R^2. However, other statistical measures should be taken into consideration as a high R^2 does not necessarily suggest causation or the fitness of the model(104).

In general, for isoconversional methods applied to TGA, an R^2 value higher than 0.90 is acceptable, indicating an excellent fitting of the model and experimental results. The R^2 values ranging from 0.80 to 0.90 are usually subject to more testing to determine whether the model is reliable. Values below 0.80 indicate poor fitting and therefore demand model revision or reconsideration. We should understand R^2 in the context of data quality, thermal process complexity, and experimental outcomes. In this way, kinetic parameters obtained by using isoconversional methods will give a real indication of the underlying thermal behavior of material (104).

The temperature dependence of the isoconversional rate in this work was determined experimentally by a TGA sequence of runs at different temperature programs. Thermal stability and degradation properties are analyzed in this study for raw palm leaves and nanocellulose materials to identify their composition and possible applications.

Figure 2.2 provides an overview of the SANAF TGA device utilized in this study, with part (a) showing the system and part (b) detailing its main components: the sample chamber for analysis, a balance for measuring weight changes, a heating element, a temperature controller, and a gas flow system for atmosphere regulation.

The TGA system, available at the laboratory of An-Najah National University in Nablus, Palestine (106), was employed to measure mass loss and heat release during the thermal decomposition process. Additionally, it includes a data acquisition unit to record weight and temperature data, supported by software for analysing and visualizing results, offering comprehensive insights into thermal behavior.

Figure 2.2

Experimental setup of a) SANAF TGA device and b) the main parts of TGA device (105)

a) 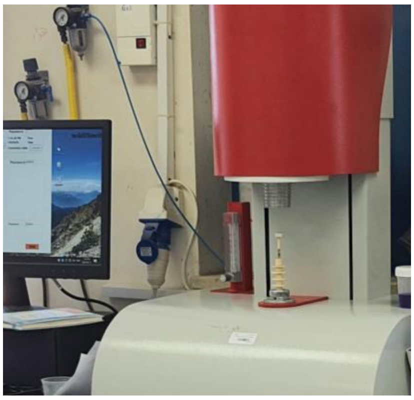

b) 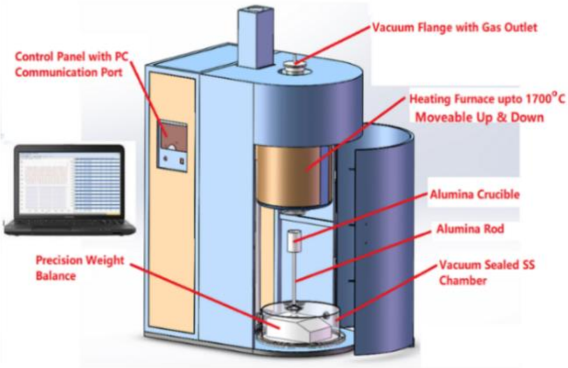

2.4.1 Sample preparation

The raw palm leaves were dried in an oven at 60°C for 24 hours to remove the water content. After drying, they were ground to achieve a uniform particle size, typically less than 1 mm. For the nanocellulose, care was taken to ensure that the extracted nanocellulose was fully dried. In each procedure, approximately 30 mg of palm leaves powder (both raw and nanocellulose) were weighed using an analytical balance, and the exact weights were recorded for analysis.

2.4.2 TGA Procedure

The TGA temperature range was adjusted from 120°C to 690°C, with an initial hold at 120°C for 10 minutes to allow for the evaporation of water from the sample. Both raw and nanocellulose palm leaves were subjected to varying heating rates from 10 to 25°C/min. The experiments were conducted under an oxygen atmosphere (O_2 flow = 50 cm^3/min) to study oxidative stability. The sample (raw palm leaves and nanocellulose) was placed in a clean, dry sample pan to ensure accurate weight measurement and prevent movement during analysis. The TGA program was initiated, heating the samples while continuously recording weight changes. Data acquisition was monitored in real-time via the software interface. The change in weight was recorded in relation to temperature. After each experiment, the device was allowed to cool to ambient temperature, and the sample pan was then cleaned with acetone and placed in a drying oven at 80°C over a period of 10 minutes.

2.4.3 Data analysis

Both raw palm leaves and nanocellulose's TGA curves were examined, with particular attention paid to the initial decrease in weight (resulting from moisture content), major degradation stages (corresponding to the breakdown of lignin, cellulose, and hemicellulose), and the remaining mass following complete degradation. Critical parameters were identified using analytical software: the temperature at which mass loss began (T-onset), the temperature of maximum rate of loss (T_max), and the total mass loss percentage, which indicated stability and composition. The TGA profiles of raw palm leaves and nanocellulose were compared, highlighting differences in thermal stability and degradation characteristics. TGA graphs generally plotted mass (y-axis) against temperature (x-axis). After the analysis was completed, the device was programmed to automatically stop heating. Microsoft Excel and Origin Pro 2024 were used to analyze loss of mass and derivative mass as functions of temperature (107).

2.4.4 DSC device

DSC quantifies the heat energy absorbed or released by a sample at constant pressure during physical or chemical transformations, offering insights into specific heat capacity and enthalpy changes associated with thermal events (108). For instance, during melting, DSC records the absorbed energy, which is vital for understanding material stability and functionality. Enthalpy changes (ΔH), representing the energy exchanged during a reaction or phase change, are measured with precision by DSC, enabling researchers to monitor heat flow and assess thermal behavior effectively (108).

Fundamental Relationships: When no physical or chemical transformations occur at a specific temperature T, the heat absorbed or released by the sample can be described by the equation (108):

$$q_p = C_p \, \Delta T \qquad [11]$$

Where: q_p represents the heat flow, C_p is the specific heat capacity, and $\Delta T = T - T_0$ denotes the temperature change, with T_0 being the initial temperature.

Assuming C_p remains constant within the relevant temperature range, the relationship between temperature and time can be represented as follows:(108):

$$T = T_0 + \alpha t \qquad [12]$$

where α represents the scan rate. Substituting this into the equation for ΔT, we obtain (108):

$$\Delta T = \alpha t \qquad [13]$$

Significant changes in the heat flow signal's behavior occur during thermal transitions:

Endothermic Processes: A decrease in the heat flow signal occurs when the sample

absorbs heat from the sensor during an endothermic event, such as melting or sublimation. An upward peak in the DSC curve is how this appears. The following are instances of endothermic transitions: decomposition, melting, sublimation, and glass transition temperature (108).

Exothermic Processes: On the other hand, the sample emits heat during exothermic procedures like oxidation or crystallization. The heat flow signal shows a downward peak, which indicates this release. Exothermic transitions include oxidation processes, solid-solid transitions, and crystallization (108).

The slope of the baseline line prior to a transition peak is indicative of the heat capacity of the substance (108):

$$\frac{dq}{dT} = C_p \qquad [14]$$

This relationship is critical for determining the thermal stability and heat capacity of materials.

The DSC curve's area under the peak also provides important information about the enthalpy change related to the transition by quantifying the energy needed for the phase transition to occur. Understanding the material's stability under various thermal conditions and describing its thermal behavior depend on this energy measurement.

Both treated and raw palm leaves samples analyzed using DSC to complement TGA results and determine if the treatment led to the production of useful chemicals and fuels. The instrument utilized for this analysis was the Discovery SDT 650 device (109).

The DSC experiment was conducted under a flow rate of 50 cm^3. min^{-1}, and varying heating rates ranging from 10 to 25 °C/min.

2.4.5 Isoconversional methods

These runs generated a correlation plot of mass and temperature, which was then transformed into α and temperature plot by measuring α as ($\Delta m/\Delta m_{tot}$) [equation (1)]. This means it indicates the mass conversion rate between any two points as well as the total change occurring over the whole of the run. Origin software was used to graph the results of all heating rates. Constant α ranges were eliminated to highlight well-separated α points for each heating rates.

Badran *et al.*, focused on sections of the α graph with constant α changes to enable more precise estimation when solving isoconversional equations (94, 110, 111). Additionally, these areas highlight critical points of change in α the graph, making it easier to identify where significant attribute variations occur. The isoconversional method cannot be used if the steps are not well-separated, as the regression lines (R^2) overlap within a specific α range hinder accurate analysis (94, 110, 111).

These regions were temperature ranges as follows:

1. For experiments conducted on raw palm leaves under an air atmosphere, the selected temperature range was 215–565°C.
2. For bleached palm leaves under similar conditions, the temperature range was adjusted to 200–490°C.

The data obtained from the TGA indicated a new range of mass, requiring an adjustment to the conversion fraction (α) based on the updated initial and final masses. The conversion fraction was recalculated using the formula introduced in Chapter 1, Equation 1 (95). Each point of the dataset was measured to compute the derivative $\frac{d\alpha}{dt}$, representing the rate of conversion over time. This calculation was performed using Microsoft Excel, specifically by applying the finite difference method (95):

$$\frac{d\alpha}{dt} = (\alpha_{i+1} - \alpha_i) / (t_{i+1} - t_i) \quad [15]$$

Given the extensive number of measurements collected from the TGA device, it was observed that there was some recurrence of values over short time intervals. To facilitate interpretation of data, a summary table was constructed at α points chosen at 0.05 intervals between α =0.10 and α =0.95. This procedure served to both reduce data redundancy and emphasize major conversion points.

To determine the rate of mass change ($\frac{dm}{dt}$), the v-lookup function in Excel was used so that the values of $\frac{dm}{dt}$ were paired with the α values in a range from 0.10 to 0.95 for the exact identification of the rate of mass loss in relation to each selected α.

Next, $\frac{d\alpha}{dt}$ was measured using the formula (95):

$$\frac{d\alpha}{dt} = \frac{-dm/dt}{m_0 - m_f} \qquad [16]$$

Where the natural logarithm of the product β $\frac{d\alpha}{dt}$ was calculated:

$$ln\ (\beta\ \frac{d\alpha}{dt})$$

The heating rate (β) was extracted from the experimental setup, and the logarithmic transformation was executed using the Excel function. The reciprocal temperature (1/T) was calculated for each α, where T in Kelvin was obtained by converting from Celsius using the equation (95):

$$T(K) = 273 + T(C°) \qquad [17]$$

In the context of isoconversional methods, terms A_α and f(α) were held constant for each specific α value to simplify the analysis.

To calculate the activation energy (E_α) using the FR method, the data for ln (β$\frac{d\alpha}{dt}$) was plotted against 1/T(K^{-1}) for every heating rate at a specific conversion (α). The slope of the best-fit line from this plot was extracted, enabling the activation energy to be calculated using the corresponding equation:

$$E_\alpha = \frac{(-slope*R)}{1000} \qquad [18]$$

where R represents the ideal gas constant. Calculating the square of the coefficient of determination (R^2) was essential for evaluating the quality of the linear fit. It provided a quantitative measure of how well the data aligned with the expected linear relationship, indicating the strength and accuracy of the fit.

For the KAS method, a separate analysis was conducted where ln $(\frac{\beta}{T^2})$ was calculated. The procedure involved plotting this value against 1/T(K) in Excel to determine the slopes of the best-fit lines. The activation energy (E_α) was again estimated using equation 18.

The R^2 values for these KAS plots were computed using the same Excel functionalities, providing insight into the reliability of the derived slopes.

Critical kinetic parameters can be effectively extracted from TGA data using both the FR and KAS approaches. As prior research has shown, these methodologies enable a greater comprehension of the kinetics and mechanisms underpinning thermal degradation processes, especially through the use of isoconversional techniques (96).

2.5 Infrared spectroscopy analysis (FTIR)

The raw, AFEX-treated, and bleached palm leaves were analyzed using FTIR spectroscopy to investigate and identify the chemical compounds as well as functional groups in the samples. The analysis was conducted using the Thermo Scientific Nicolet iD3 ZnSe Attenuated Total Reflectance (ATR) device, which was available at An-Najah National University (Nablus, Palestine) (112).

The base of infrared spectroscopy is the absorption of infrared light by molecules at wavelengths characteristic to vibrational frequencies of their bonds, which lead to stretching, bending, and twisting of atoms within the molecule (113).

In order to increase the precision of the spectral data, the samples were thoroughly ground into very fine powder using mortar and pestle before the analysis. A very small amount of the powdered material was carefully loaded into the ATR cell using a spatula. The sample was put in front of the infrared source to maximize contact with the radiation.

The produced analog signal was transformed into a spectrum and further processed using specialist software after the radiation exposure. The obtained spectrum enabled the identification of characteristic peaks relative to various chemical compounds and functional groups present in the samples. This provided very important information about structural characteristics and the chemical composition of palm leaves that allowed deeper insight into the effects of the treatment procedures applied.

2.6 Scanning electron microscope (SEM)

The nano adsorbent SEM images were obtained on a Nova Nano SEM 450 field emission instrument (114). Voltage acceleration of 5 kV was used in the microscope to enable high-resolution imaging, which is quite important in observing the intricate structural features of the nano-adsorbent (114).

In addition, the SEM was equipped with an Energy Dispersive X-ray (EDX) analyzer from Bruker, which allowed the detailed elemental analysis of the composition of the adsorbent. The SEM scanned the surface of the sample with a high-energy electron beam, thereby producing a number of signals based on the interaction between the electron beam and the sample. These included back scattered electrons, which developed contrasts due to atomic number differences and hence provided surface structure information, and secondary electrons, which gave topographical information (23).

In this way, the combination of SEM imaging and EDX analysis provided complete knowledge about morphology and chemical composition, which is very important in understanding the potential applications of the nano adsorbent in adsorption processes. EDX analysis allowed for the identification and quantitative elemental composition of the sample, identified by the X-rays emitted upon the excitation of electrons (115).

High-resolution imaging of surface features with great accuracy of elemental composition was possible with SEM-EDX, thus enabling detailed investigations into microstructures and characteristics of materials. Moreover, this technique has been highly versatile, owing to its extensive use in materials science, nanotechnology, biology, geology, and numerous industrial fields for non-destructive investigations at micro and nanoscales, which provide critical data on how to optimize material design and functionality (116).

Chapter Three

Results and Discussions

3.1 Experimental thermochemical analysis, using isoconversional methods

The experimental component of this study generated comprehensive thermochemical and kinetic data. Each parameter was systematically graphed and tabulated to illustrate their interrelationships and the significance of each in the context of the isoconversional methods applied. These methods were utilized in accordance with the formulations provided in equations [1-8, 16-18], allowing for a detailed analysis of the thermal behavior of the samples. The resulting data not only elucidates the kinetic parameters but also provides valuable insights into the fundamental mechanisms driving the thermal processes.

TGA of raw and bleached palm leaves under oxidative conditions revealed distinct degradation profiles that varied with different heating rates. Figure 3.1 illustrates the TGA curves for raw and bleached palm leaves at temperatures ranging from 120 to 690 °C with heating rates of 10, 15, 20, and 25 °C/min.

Figure 3.1 (a) raw palm leaves illustrates how the raw palm leaves' decomposition began at about 215 °C and finished around 565 °C. The decomposition temperatures were notably raised by greater heating rates, suggesting a change in the biomass's thermal stability and degradation dynamics.

And figure 3.1 (b) bleached palm leaves: In contrast, the decomposition of bleached palm leaves initiated at a slightly lower temperature of 200 °C and finished at about 490 °C. A significant observation in this analysis was the overlap between 375 °C and 416 °C, suggesting the occurrence of two concurrent decomposition mechanisms during this temperature range. The reduced thermal degradation temperatures of bleached palm leaves highlight the efficiency of the bleaching process in altering their thermal properties. Specifically, bleached samples began to decompose at 200 °C, while raw palm leaves started at 215 °C, and the bleached samples completed their decomposition at 490 °C compared to 565 °C for the raw samples.

Bleaching of palm leaves reduced thermal stability significantly because it removed lignin and hemicellulose, both of which contribute to raw biomass's structural integrity and thermal resistance (117). As a result, bleached samples decomposed faster, beginning and ending at lower temperatures. This enhanced thermal profile suggests that bleached palm leaves are especially useful for bioenergy applications that need rapid and efficient decomposition.

Figure 3.1

TGA curves of raw and bleached palm leaves under O_2 at different heating rates

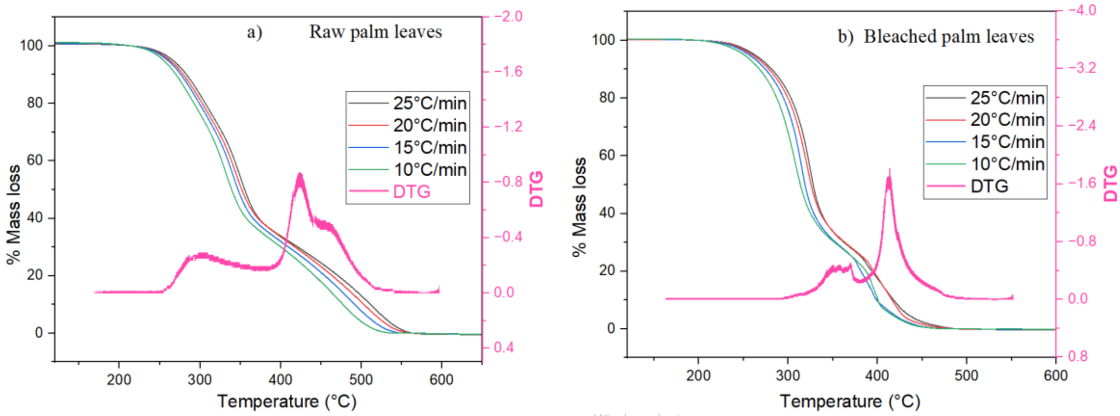

Note: a) raw and b) bleached palm leaves under O2, at different heating rates of 10, 15, 20, and 25 °C/min

Figure 3.2 presents the temperature-dependent conversion (α) of raw and bleached palm leaves during decomposition under oxidative conditions.

Figure 3.2 (a) shows that with an increase in the heating rate, the decomposition temperature of raw palm leaves increased, which means thermal stability has been improved, and hence, more energy is needed to start the degradation of raw palm leaves at higher heating rates.

In the case of bleached palm leaves, figure 3.2 (b) depicts that shifting of the decomposition process to a higher temperature occurs with an increase in the heating rate. Importantly, the bleached samples present clear separation within the conversion range of α between 0 and 0.53. It goes to follow that such clearly separated curves will have more homogeneous and predictable thermal behavior for bleached palm leaves at the noted conversion levels—meaning a more effective and consistent mechanism of decomposition than for their raw counterpart. These observations bring out the effects of chemical treatment, besides heating rate, on the characteristics of thermal degradation for palm leaves and provide information necessary in the optimization of their uses in various applications.

Figure 3.2

Degree of conversion (α) as a function of temperature at different heating rates in an O_2 atmosphere

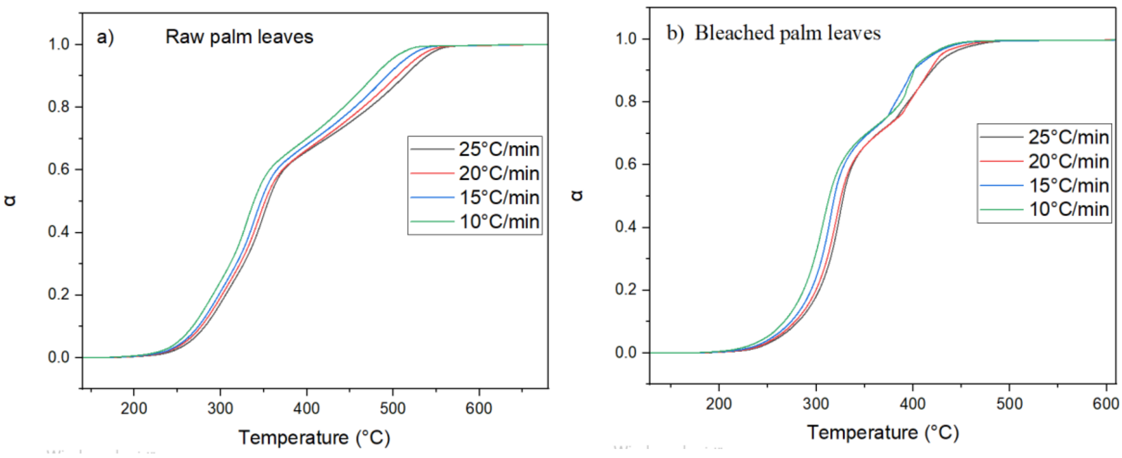

Note: *Conversion degree (α) as a function of temperature, for various heating rates, in O_2 atmosphere of the a) raw palm leaves and b) bleached palm leaves oxidative decomposition.*

Figures 3.1 and 3.2 show how chemical treatment and heating rate influence thermal degradation. By adjusting these factors, it is possible to optimize energy conversion conditions, thereby enhancing energy production and improving processing efficiency.

The study employed Arrhenius plots to examine the oxidative decomposition kinetics of raw and bleached palm leaves, as explained in chapter 2. The results highlight the impact of chemical treatment, which alters structural and chemical properties, and reveal significant methodological differences between the FR and KAS methods as shown in figures 3.3 and 3.4.

Figure 3.3 (a) depicts the Arrhenius plot for the oxidative decomposition of raw palm leaves utilizing the FR method, illustrating the temperature range from 215 to 565 °C. The plot illustrates the relationship defined by the Arrhenius equation 4 (as mentioned in Chapter 1).

This linear representation of the Arrhenius equation enables the calculation of activation energy from the slope of the plot, as mentioned in equation 18. This indicates that the decomposition process follows a single kinetic mechanism over this temperature range, providing insight into the thermal behavior of raw palm leaves during oxidative decomposition.

Figure 3.3 (b) displays the Arrhenius plot for the oxidative decomposition of bleached

palm leaves at temperatures ranging from 200 to 490 °C. The observed gap of this plot is attributed to the overlap region during decomposition, indicating the presence of multiple kinetic mechanisms operating within this temperature range. This suggests that the decomposition of bleached palm leaves involves more complex mechanisms compared to raw palm leaves.

Figure 3.3

Arrhenius plots of the oxidative decomposition using the FR method

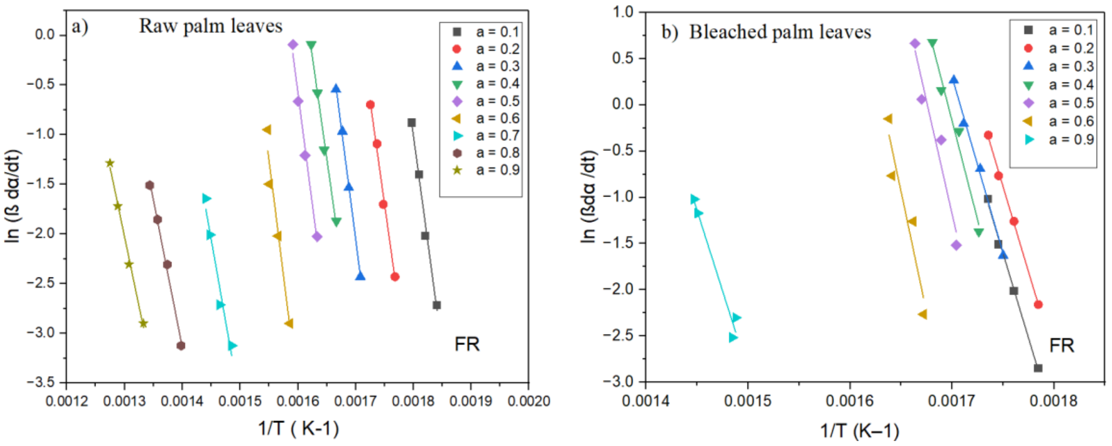

Note: a) Raw and b) bleached palm leaves in O_2 using the FR method.

By contrast, the oxidative decomposition of bleached palm leaves (b) starts at lower temperatures than that of raw palm leaves (a), which means that the thermal stability of the material is reduced during the course of the bleaching process. This reflects the influence of chemical treatment on decomposition behavior and points out that in oxidative processes, bleached palm leaves might exhibit higher reactivity.

Bleaching alters the structural and chemical properties of palm leaves, thereby affecting their thermal decomposition behavior. It was apparent that bleached palm leaves exhibited enhanced reactivity and may find potential applications in processes requiring faster decomposition, for example, in bioenergy production (118).

Figure 3.4 (a): Arrhenius plot obtained for the raw palm leaves oxidative decomposition, by KAS method, in a linear trend within the temperature interval from 215 to 565 °C. The linearity of this plot reflects that the kinetic behavior is uniform in the given temperature interval and hence the activation energy associated with the decomposition process could be calculated effectively.

Figure 3.4 (b) presents the Arrhenius plot for bleached palm leaves in the temperature range of 200-490 °C, showing a complex profile as evidenced by the presence of gaps. This is indicative of more than one kinetics mechanism superimposing in the decomposition; hence, this reflects the complex nature of the thermal behavior of chemically treated materials.

Figure 3.4

Arrhenius plots of the oxidative decomposition using the KAS metho

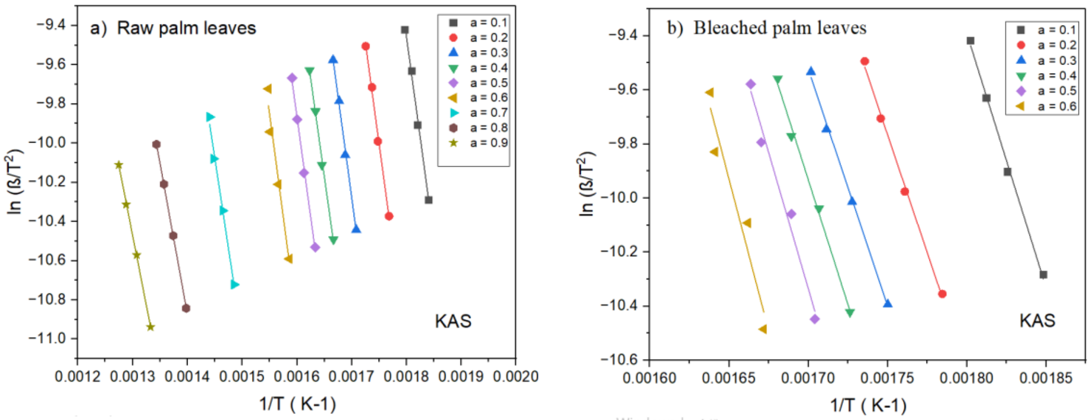

Note: The Arrhenius plots of the oxidative decomposition for a) Raw and b) bleached palm leaves in O_2 using the KAS method

Figures 3.3 and 3.4 show the better capability of FR method in analysing the kinetics of oxidative decomposition compared to that from the KAS method. The Arrhenius plots obtained using FR method provide more complete and deep information regarding the oxidative decomposition process. More particularly, the FR method captures the plots show distinct overlaps, indicating that more than one reaction pathway occurs simultaneously, hence giving a better representation of the complexities of the decomposition process. This gives a better representation of the kinetic parameters involved in the process.

By contrast, though the KAS method is a useful analytical tool, it seems to be less capable of capturing complex interactions properly in the oxidative decomposition of palm leaves, especially for bleached samples. Gaps in the KAS plots suggest a failure of capturing the full range of reactions during decomposition, which can be an obstacle to gaining a full understanding of the mechanisms underlying the process. On the other hand, the FR method fits all those applications for which reactivity and decomposition behavior must be nuanced-especially biomass conversion and waste management. For instance, several studies, including works by I. Badran et al., proved that the FR method surpasses the KAS method in analysing such complex materials as chemically treated bleached biomass (94, 96).

Figure 3.5 presents the variation of activation energy vs. the extent of conversion (α) for both methods. It can be observed that the FR method yields a big range of activation energies (300-440 kJ/mol) reflecting more variation and multiple mechanisms of reaction involved. This suggests that the FR method is more sensitive to the complexities of the decomposition process, especially for chemically modified materials such as bleached biomass that may have more complicated degradation pathways.

Figure 3.5

Variation of activation energy (E_α) for the oxidative decomposition of palm leaves in O_2 as a function of conversion (α)

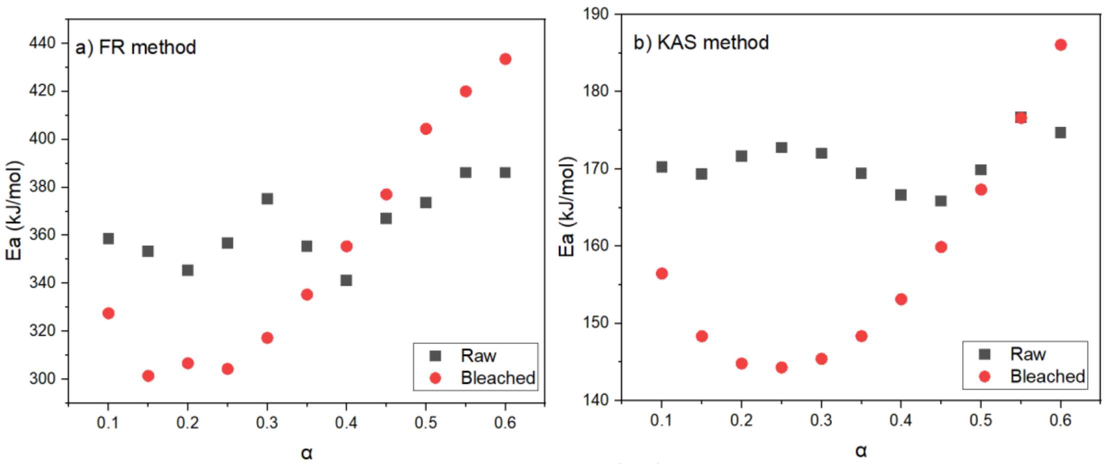

Note: (α) by using a) FR and b) KAS methods.

On the other hand, the KAS method possesses an activation energy profile which is much more stable in the range of 140-190 kJ/mol and does not show such big variations throughout the conversion range. Such a consistent trend suggests that the KAS method models a single-step, simpler decomposition process that cannot fully describe materials with multiple reaction pathways. This contrast was pointed out in earlier studies by I. Badran et al., emphases the advantage of the FR method for the analysis of materials with heterogeneous reaction stages such as chemically treated biomass (94, 96).

Understanding the different activation energies at various conversion extents is critical for optimizing biomass conversion processes and improving energy production and waste management strategies. The FR method is more sensitive to the conversion extent and can capture more complex decomposition pathways, while KAS may work better for a more consistent simple model.

3.2 FTIR analysis

Figure 3.6 shows the FTIR analysis of palm leaves in various states (raw, AFEX-treated, and bleached) provides insight into the chemical composition and structural changes that occur during processing. Each treatment reveals distinct spectral characteristics that reflect the chemical transformation of the material.

Figure 3.6 (a) the FTIR spectrum of raw palm leaves displays complex and broad peaks, indicating the presence of bulk molecules. Due to the intricate composition of the raw leaves, which includes a combination of cellulose, hemicellulose, lignin, and other plant components, it is challenging to identify specific molecular peaks. There is a broad O-H stretching band (~3300-3500 cm^{-1}): This broad peak is indicative of hydrogen-bonded hydroxyl groups, common in the hydroxyl-rich structure of cellulose and hemicellulose, also from moisture present in the raw leaves.

C-H stretching (2850-2950 cm^{-1}) the signals in that region suggest the existence of aliphatic compounds, typically associated with the cellulose as well as hemicellulose components. The existence of lignin is reflected in the aromatic C=C stretching bands (~1600 cm^{-1}), which are generally observed in this region. And C-O-C and C-O stretching (1000-1200 cm^{-1}), these peaks are due to the polysaccharide backbone of cellulose and hemicellulose, showing the presence of glycosidic linkages.

This spectrum reflects the complex, the bulk molecular structure and multi-component nature of the raw palm leaves, where peak overlaps obscure clear identification of individual functional groups.

Figure 3.6 (b) shows the FTIR of AFEX-treated palm leaves, in this spectrum the peaks become more distinct compared to the raw material, indicating partial decomposition and transformation due to the AFEX process.

The large peak at 3300-3500 cm⁻¹ indicates O-H stretching vibrations from hydroxyl groups found in cellulose and hemicellulose. The existence of that peak indicates the retention of hydroxyl groups following AFEX process.

The peak at 2900 cm⁻¹ is connected to C-H stretching, most likely from residual cellulose or lignin.

Figure 3.6

FTIR spectra of a) raw, b) AFEX, and c) bleached palm leaves.

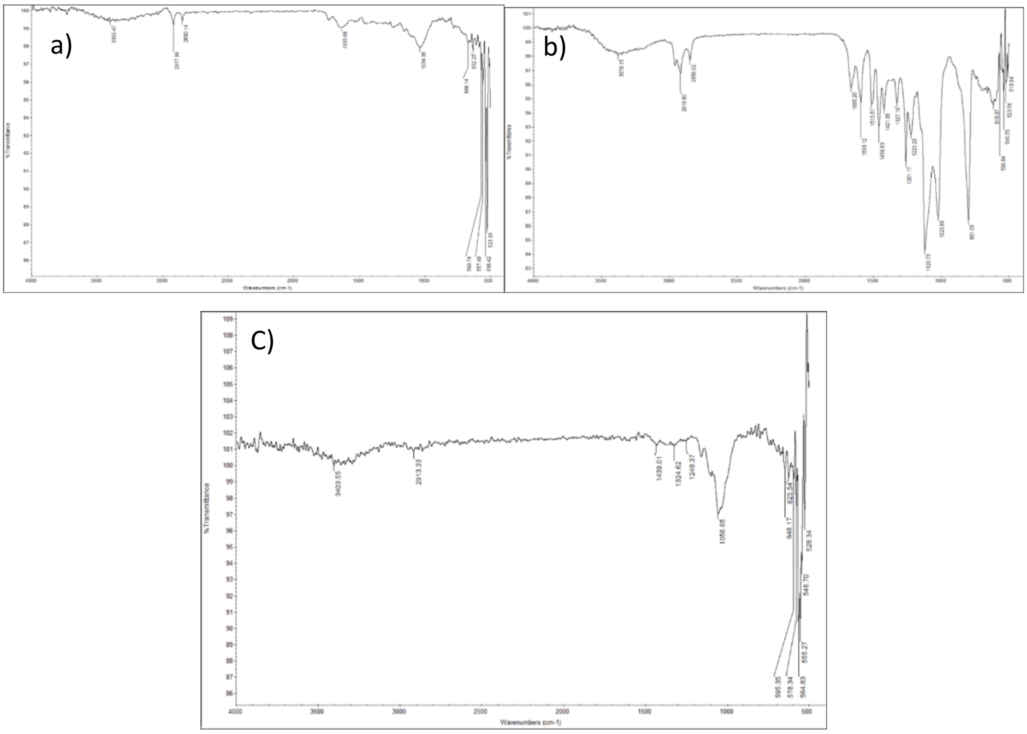

Note: FTIR spectra of a) raw, b) AFEX, and c) bleached palm leaves.

As observed in figure 3.6 (b), the carbonyl (C=O) stretching peaks at 1600-1700 cm⁻¹ may be caused by lignin or fatty acid residues that remain after AFEX treatment. These peaks correspond to partial retention of lignin and other carbonyl-containing molecules.

Peaks around 1000-1200 cm⁻¹ represent the C-O-C and C-O-H vibrations seen in cellulose and hemicellulose structures. The AFEX method may have eliminated or decreased some hemicellulose-specific characteristics. However, peaks about 1730 cm⁻¹ (typically linked with acetyl groups in hemicellulose) are less strong, indicating partial decomposition.

The AFEX treatment clarifies the functional group peaks, making it easier to identify and analyze cellulose, lignin, and fatty acids. This sharper spectrum is important for validating structural alterations that improve the material's thermal characteristics, making it potentially viable for applications requiring greater heat resistance.

Figure 3.6 (c) shows the purified cellulose in the bleached palm leaves' FTIR spectrum, which displays distinctive peaks related to cellulose's chemical structure. The key characteristics that can be discerned from the FTIR spectrum are broken down as follows:

O-H stretching (broad peak) which is the hydroxyl (O-H) groups in cellulose are characterized by a broad peak that lies between 3200 and 3500 cm^{-1}. The prominence of this peak suggests a high concentration of hydroxyl groups, which is characteristic of the structure of cellulose.

C-H stretching vibrations, which are also frequent in cellulose, can be linked to the tiny peaks at about 2900 cm^{-1}.

The polysaccharide structure of cellulose is further highlighted by the peaks about 1000–1200 cm^{-1}, which are linked to C–O–C (ether) and C–O–H stretching vibrations of the cellulose backbone.

In contrast to raw or untreated biomass, the absence of notable peaks associated with lignin-typical aromatic rings or hemicellulose-specific peaks at around 1600 cm^{-1} and 1730 cm^{-1} indicates that lignin and hemicellulose have been eliminated. The bleaching process is characterized by this purification.

Because it reduces interference from other substances like lignin as well as hemicellulose, the pure cellulose structure is perfect for applications that call for a high cellulose concentration. Comparing this refined substance to raw or untreated samples may reveal more consistent chemical behavior, stability, and modification potential (119).

So, an FTIR analysis in Figure 3.6 indicated distinct chemical changes produced by bleaching and AFEX treatment. Raw samples included complicated and overlapping peaks that indicated the presence of cellulose, hemicellulose, and lignin. After treatment, FTIR spectra showed sharper peaks, particularly in bleached samples, indicating a purifying impact with higher cellulose content. The decrease in lignin and hemicellulose-related peaks was consistent with thermal decomposition data, which showed that bleached samples were less thermally stable.

3.3 DSC analysis

DSC is employed to assess the thermal properties of materials by tracking the heat flow resulting from changes in temperature. This investigation compares the thermal behavior of raw (light green curves) and bleached (red curves) palm leaves at four distinct heating rates: 10°C/min, 15°C/min, 20°C/min, and 25°C/min as shown in the figure 3.7. Bleaching frequently modifies the lignocellulosic structure, which affects thermal stability also the decomposition rates.

Raw palm leaves (light green curves) the raw samples decompose at a higher temperature than the bleached samples, demonstrating increased thermal stability due to the untreated material's intact lignocellulosic structure.

The bleached samples (red curves) the decomposition at somewhat lower temperatures than the raw samples, most likely because the bleaching procedure eliminates structural components (like lignin), leaving the material more prone to decomposition, as identified in FTIR analysis (figure 3.6).

The bleached palm leaves consistently show larger areas under the DSC curves at each heating rate, indicating a greater heat release. This is likely due to the enhanced reactivity from the removal of stable lignin structures, which exposes more reactive cellulose components.

In contrast, the raw palm leaves exhibited smaller areas under the DSC curves, suggesting a more stable structure that requires more energy to decompose, resulting in a slower heat release.

Figure 3.7

DSC curves for raw and bleached palm leaves at different heating rates

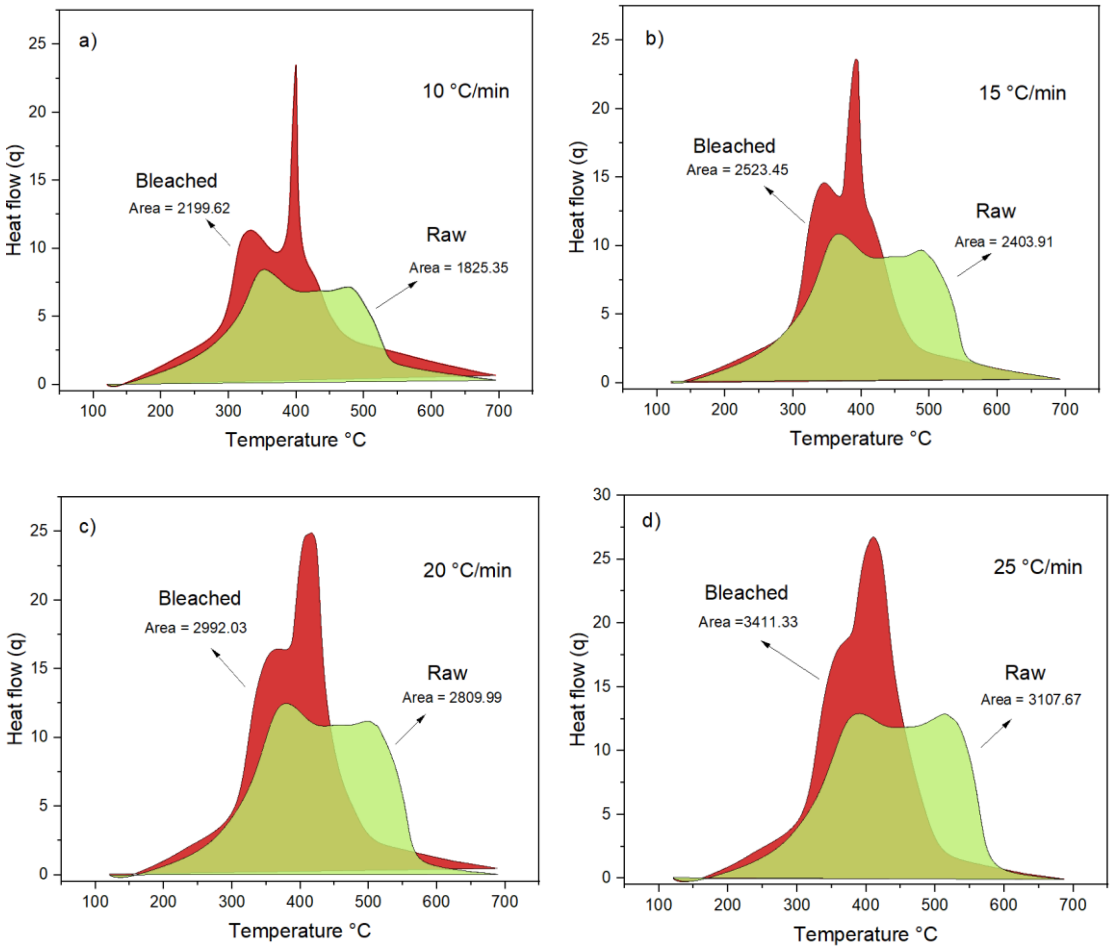

Note: DSC curves for raw and bleached palm leaves at a) 10 °C/min b) 15 °C/min c) 20 °C/min and d) 25 °C/min

At a heating rate of 10°C/min (Figure 3.7(a)), both raw and bleached palm leaves show lower heat release, suggesting a slower and more controlled decomposition process. When the heating rate increases to 15°C/min (Figure 3.7(b)), the heat release rises for both samples, with the bleached sample releasing more heat than the raw sample. As the heating rate reaches 20°C/min (Figure 3.7(c)), heat release accelerates, and the bleached sample undergoes the most significant decomposition. At the highest heating rate of 25°C/min (Figure 3.7(d)), the heat release is maximized for both samples, with the bleached sample releasing 3411.33 a.u., compared to 3107.67 a.u. for the raw sample. This demonstrates that higher heating rates facilitate faster thermal decomposition, especially in bleached materials.

Across all heating rates, bleached samples consistently display higher heat values than raw samples, as seen by bigger regions under DSC curves. This suggests that bleaching not only reduces thermal stability but also enhances calorific value in palm leaves, perhaps making them more appropriate for bioenergy applications. These observations complement the thermal decomposition profiles (e.g., Arrhenius and activation energy analyzes), where bleached samples displayed reduced thermal stability and increased susceptibility to decomposition.

According to the DSC investigation, bleaching impacts palm leaves thermal characteristics, diminishing thermal stability while increasing total heat loss. The lower decomposition start temperature in bleached samples is related to structural changes caused by the bleaching process, whereas the larger area under the curve indicates higher heat production. These modifications are significant to bioenergy applications where larger calorific values are advantageous (120).

The impact of heating rate emphasizes the relevance of processing conditions. Faster heating rates allow for faster decomposition, which is useful in applications that need rapid thermal processing, but slower heating rates provide for a better view of gradual thermal transitions.

The DSC results are also relevant to the thermal decomposition kinetics shown in Figures 3.3, 3.4, and 3.5. Bleached samples release more energy, which confirms Arrhenius' observations of increased reactivity due to overlapping reaction pathways in chemically treated materials. This is supported by FTIR spectra, which show the exposure of reactive cellulose following the removal of stabilizing components such as lignin and hemicellulose.

So, The DSC study revealed that bleached palm leaves released more heat at all heating rates, indicating higher reactivity due to increased cellulose exposure and loss of stabilizing lignin structures. This energy release makes them a desirable feedstock for energy-intensive applications. Both raw and bleached samples decomposed more quickly at higher temperatures, but bleached samples consistently produced more heat, making them suitable for rapid thermal processing.

3.4 SEM analysis

The SEM images in Figure 3.8 illustrate the structural differences between raw and bleached palm leaves at the microscopic level.

Figure 3.8 (a) shows the SEM image of raw palm leaves indicating a very irregular surface with no evidence of a fibrous structure. Particles possess jagged edges and rough texture, indicating the dense and compact matrix. The lack of well-defined fiber formation is indicative that the raw material is more rigid and structurally complicated. The irregularities in shape and roughness of surfaces because of some natural, untreated components of palm leaves, as lignin, hemicellulose, and other plant-based matter that may lend rigidity, causing such inconsistency.

On the other hand, Figure 3.8 (b) shows the SEM image of bleached palm leaves, exhibiting a clear fibrous structure. The fibers become elongated, taking regular shape and forming a network of smooth, interwoven strands. Such a transformation from a rough, non-fibrous to a structured, fibrous arrangement is most likely due to the bleaching method, which removes lignin and other binding components. This provides more evidence that the bleaching process tends to improve the material toward a more organized, open structure, maybe with smoother particle surfaces, so increasing porosity and consequently reactivity in subsequent applications. The change might have a significant impact on mechanical characteristics, namely thermal reactivity, as evidenced by variations between raw and bleached samples based on activation energy measured during thermal decomposition.

The structural changes visible in SEM pictures correspond to the findings of thermal analyzes. For example, larger heat fluxes are recorded by the DSC method in bleached materials due to their higher porosity, which enables faster heat transmission and reaction rates. This corresponds to the increased calorific potential and reduced thermal stability of bleached samples, as evidenced from DSC and FTIR results shown in Figures 3.6 and 3.7.

The removal of lignin, identified by FTIR and confirmed by SEM, would increase the suitability because its thermal reactivity and energy release on decomposition is greatly improved to be used in bioenergy applications.

Figure 3.8

The SEM images of a) raw and b) bleached palm leaves

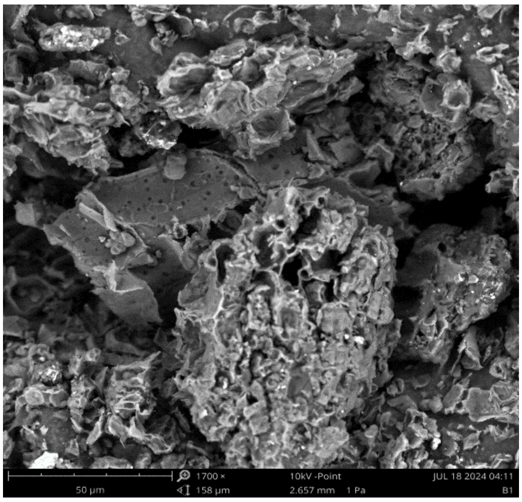

a)

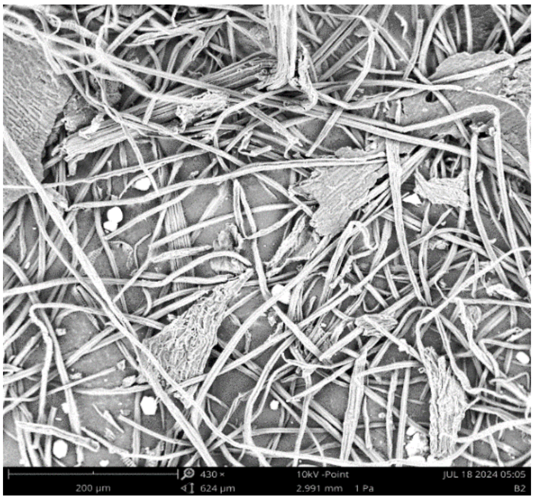

b)

Note: The SEM images of a) raw and b) bleached palm leaves.

Such structural and chemical changes further show how bleached palm leaves adapt to energy-intensive processes, aligning with the greater mission of enhancing biomass for utilization in bioenergy applications. Joint investigations by FTIR, DSC, and SEM provide an overview of how chemical treatment changes material properties to achieve these results.

3.5 Kinetic modelling and determination of the kinetic triplet

The isoconversional method serves as a tool to identify the reaction model and determine kinetic parameters, including A, $\Delta H^{\neq}$, $\Delta S^{\neq}$, and $\Delta G^{\neq}$. By utilizing the Friedman equation (Eq. 7), a plot of the left-hand term of Eq. 7 (ln ($\beta_i \frac{d\alpha}{dT}$) against ln f(α)) is created for various known f(α) models. According to Eq. 7, the slope of this linear relationship is expected to be unity (95). Experimental data for raw and bleached palm leaves reactions under O_2 were used to apply this fitting approach across different reaction models, as previously outlined in references (95). The results of these linear fits are provided in Table 1. While the fittings were performed at various α values, the most accurate results corresponded to α=0.25. The best fit was achieved using the three-dimensional diffusion model, expressed by:

$$f(\alpha) = \frac{3}{2}(1 - \alpha)^{\frac{2}{3}}\,[1 - (1 - \alpha)^{1/3}]^{-1} \qquad [19]$$

Since the y-intercept of the linear fit corresponds to ln(A_α f(α)), the pre-exponential factor A_α was computed by substituting the intercept values into this relationship. The unimolecular pre-exponential factor A_α can be expressed as (108):

$$A_{uni} = \left(\frac{ek_BT}{h}\right) e^{\Delta S^{\neq}/\mathrm{R}} \quad [20]$$

here, e is Euler's number (2.7183), k_B is Boltzmann's constant, h is Planck's constant, and R is the ideal gas constant. Rearranging the equation 20 allows for calculating the entropy of activation $\Delta S^{\neq}$ (108):

$$\Delta S^{\neq} = R \left(ln \frac{Ah}{ek_BT}\right) \quad [21]$$

Additionally, the enthalpy $\Delta H^{\neq}$ and Gibbs free energy $\Delta G^{\neq}$ of activation can be derived using the following equations (108):

$$E\alpha = \Delta H^{\neq} + RT \quad [22]$$

$$\Delta G^{\neq} = \Delta H^{\neq} - T\Delta S^{\neq} \quad [23]$$

Table 1

Kinetic parameters were determined by combining the Friedman equation with model fitting at α=0.25, for raw and bleached palm leaves

Samples	Raw	Bleached
T/°C	302.60	293.3
f(α)	$f(\alpha) = \frac{3}{2}(1-\alpha)^{\frac{2}{3}}[1-(1-\alpha)^{1/3}]^{-1}$	
Slope	4.814	1.664
R^2	0.9947	0.9904
A_α/ s^{-1}	1.4×10^{30}	1.4×10^{26}
$\Delta S^{\neq}$ J/mol·K	318.5	241.9
$\Delta H^{\neq}$ kJ/mol	351.9	299.6
$\Delta G^{\neq}$ kJ/mol	168.5	162.6

The kinetic study reveals notable differences between raw and bleached palm leaves under oxidative (O_2) conditions. At 25% conversion, raw palm leaves exhibit a considerably larger pre-exponential factor (A_α) of 1.4×10^{30} s^{-1}, compared to 1.4×10^{26} s^{-1}

for the bleached samples. This difference can be attributed to the bleaching procedure, which alters the molecular structure and reaction pathways, leading to a significant reduction in A_α for the bleached sample. Additionally, the activation entropy ($\Delta S^{\neq}$) shows a similar trend. Raw palm leaves have a higher $\Delta S^{\neq}$ value of 318.5 J/mol·K, whereas bleached samples have a lower value of 241.9 J/mol·K. The greater $\Delta S^{\neq}$ for raw palm leaves suggests more molecular disorder and complexity in the transition state, which is reduced during the bleaching process. This highlights how the pre-treatment simplifies the material and potentially makes its reactivity more uniform.

Table 1 presents a comprehensive comparison of the thermodynamic parameters $\Delta H^{\neq}$ and $\Delta G^{\neq}$ for raw and bleached palm leaves under oxidative conditions. Raw palm leaves exhibit a significantly higher enthalpy of activation ($\Delta H^{\neq}$) of 351.9 kJ/mol, compared to 299.6 kJ/mol for the bleached samples. This difference is related to the dependence of $\Delta H^{\neq}$ on the activation energy (E_α), as described by Eq. 22. The higher $\Delta H^{\neq}$ for raw palm leaves indicates that more energy is required to achieve the transition state, likely due to the structural complexity and stronger molecular interactions inherent in the untreated biomass. On the other hand, the bleached palm leaves, with their simplified structure, require less energy for decomposition, as reflected in the lower $\Delta H^{\neq}$ value.

Despite these significant differences in $\Delta H^{\neq}$, the Gibbs free energy ($\Delta G^{\neq}$) values for both raw and bleached palm leaves were relatively similar. The raw palm leaves had $\Delta G^{\neq}$ = 168.5 kJ/mol, while the bleached sample showed a slightly lower value of 162.6 kJ/mol. According to Eq. 23, $\Delta G^{\neq}$ is influenced by both $\Delta H^{\neq}$ and the activation entropy ($\Delta S^{\neq}$). The higher $\Delta S^{\neq}$ for raw palm leaves results in a smaller magnitude for the $-T\Delta S^{\neq}$ term, which compensates for the larger $\Delta H^{\neq}$, leading to a similar $\Delta G^{\neq}$ value for both samples.

Both raw ($\Delta H^{\neq}$ = 351.9 kJ/mol) and bleached ($\Delta H^{\neq}$ = 299.6 kJ/mol) palm leaves, the higher $\Delta H^{\neq}$ for raw palm leaves indicates a more energy-intensive process due to the intact lignocellulosic matrix, which is more resistant to thermal degradation. In contrast, the bleached palm leaves decompose more readily, requiring less energy input for the same process.

Chapter Four

Conclusions

4.1 Conclusion

This study examines the effects of chemical treatment on the thermal stability, the decomposition kinetics, and structural composition of palm leaves. The results show that bleaching significantly impacts thermal stability while increasing reactivity, as showed by lower the decomposition temperatures, more variability in activation energies, and an enhanced caloric value. These changes show a trend toward more efficient thermal decomposition with higher energy release capacity.

FTIR and SEM structural analysis showed that pre-treatment disrupted the lignocellulosic matrix and, therefore, simplified the biomass structure. These structural reconfigurations increase reactivity and make biomass more suitable for energy applications like biofuel production, co-firing, and other thermal energy purposes.

The kinetic study shows a considerable difference between the raw and the bleached leaves of palm. The activation enthalpy and entropy for raw palm leaves are greater, hence, more suitable for high-energy applications requiring more heat production, while the decomposition requires much energy. Bleached leaves have lower activation energies and higher reactivity, hence ideal for energy-effective processes such as biofuel production since they require less energy for processing. The study identifies that the most important step in the development of biomass for particular fuel applications is pre-treatment in a way to balance energy efficiency with the output.

Moreover, the findings indicate the need to apply proper kinetic modelling methods, such as the FR method, which is capable of catching the real complexity of the overlapping reaction pathways in chemically treated biomass. These results set a foundation for enhancing pre-treatment strategies and kinetic modelling techniques with a view to fully realizing biomass' promise as sustainable energy sources.

4.2 Limitations

The kinetic analysis applied in this study is based on isoconversional methods, including FR and KAS. These methods assume of homogeneity in the reaction, which is not the case in biomass. Biomass is heterogeneous in nature and comprises different components such as cellulose, lignin, and hemicellulose that do not degrade at the same rate or by the same mechanism. This therefore means that the assumption of homogeneous response over-simplifies the decomposition process. Because of this, the model probably will not allow the intricacy and diversity of reactions that would occur in any real biomass sample to be brought into view with regard to how such a complex process proceeds.

While the FR method was more sensitive in finding overlapping reaction mechanisms (i.e., when several decomposition processes were occurring at the same time), employing it alone may not provide a complete knowledge of these complicated events. Complementing it with other kinetic models or advanced techniques (such as in situ spectroscopy) may offer a more detailed and accurate picture of how these processes occur. Essentially, while the FR method provided important insights, it may not be sufficient in itself to properly capture the complexities of biomass decomposition.

4.3 Recommendations

Using Real-Time, In Situ Techniques: While FTIR analysis was useful in this work, future research might benefit from in situ or real-time FTIR to track chemical changes as they occur during decomposition. When combined with mass spectrometry or other real-time spectroscopic techniques, this approach has the potential to deepen the mechanistic understanding of each phase of decomposition and reveal transient intermediates, providing more precise insights into the thermal behavior and complex reaction pathways of heterogeneous biomass.

Future tests should explore a larger variety of heating rates and conditions, such as oxidative atmospheres that resemble combustion or gasification, to make the work more practical in industrial settings. Testing at different heating rates and environmental conditions, such as in pilot reactors, would provide a better knowledge of thermal stability and decomposition in real industrial settings.

Real-time techniques like synchrotron-based X-ray imaging or SEM might improve our understanding of how the palm leaves structure changes during decomposition. This might give visual insights into the decomposition of cell walls and the release of volatile components, providing structure to the thermal and kinetic data sets.

To bridge the gap between laboratory and industry applications, studies in pilot reactors under conditions that are more similar to industrial settings would help confirm laboratory findings on a wider scale. This would verify that the decomposition behavior and energy release features seen in lab conditions are constant and useful in real-world, large-scale applications.

List of Abbreviations

Abbreviation	Meaning
α	Extent of the Reactant Conversion
AFEX	Ammonia Fiber Expansion
A_α	Pre-exponential Factor
ATR	Attenuated Total Reflectance
B	Heating Rate
BET	Brunauer, Emmett, and Teller Theory
BMP	Biochemical Methane Potential
C_p	Heat Capacity
ΔG	Gibbs Free Energy Change
ΔH	Enthalpy Change
Δm	Current Mass Change
Δm_{tot}	Total Mass Change
ΔS	Entropy Change
DSC	Differential Scanning Calorimetry
E_α	Activation Energy
EDX	Energy-Dispersive X-ray Spectroscopy
EJ	Exajoule
$f(\alpha)$	Reaction Model Function
FR	Friedman Method
FTIR	Fourier-Transform Infrared Spectroscopy
g/mol	Grams per mole
i	Identity of the Temperature Program
K	Kelvin
KAS	Kissinger–Akahira–Sunose Method
k(T)	Reaction Rate Constant

kJ/mol	Kilo Joules per mole
M	Mass
m_f	Final Mass
M_0	Initial Mass
MPa	Megapascal
PAH	Polycyclic Aromatic Hydrocarbons
PCDD	Polychlorinated Dibenzo-p-Dioxins
q_p	Heat Flow
R	Gas Constant
R^2	Square Coefficient of determination
SEM	Scanning Electron Microscopy
T	Temperature
T_0	Onset Temperature
TEMPO	(2,2,6,6-Tetramethylpiperidin-1-yl)oxyl
T_f	Final Temperature
T_i	Initial Temperature
TGA	Thermogravimetric Analysis
XRD	X-Ray Diffraction
°C	Degrees Celsius/ Degrees Centigrade

References

1. Mishra K, Siwal SS, Nayaka SC, Guan Z, Thakur VK. Waste-to-chemicals: Green solutions for bioeconomy markets. Science of The Total Environment. 2023;887:164006.

2. Sharma B, Vaish B, Monika, Singh UK, Singh P, Singh RP. Recycling of organic wastes in agriculture: an environmental perspective. International journal of environmental research. 2019;13:409-29.

3. Nugraha MG, Mozasurya ED, Hidayat M, Saptoadi H. Evaluation of combustion characteristics in biomass residues open burning. Materials Today: Proceedings. 2023;87:45-50.

4. Abubakar IR, Maniruzzaman KM, Dano UL, AlShihri FS, AlShammari MS, Ahmed SMS, et al. Environmental sustainability impacts of solid waste management practices in the global South. International journal of environmental research and public health. 2022;19(19):12717.

5. Niinemets Ü, Peñuelas J. Gardening and urban landscaping: significant players in global change. Trends in plant science. 2008;13(2):60-5.

6. Ramaiah M, Avtar R. Urban green spaces and their need in cities of rapidly urbanizing India: A review. Urban science. 2019;3(3):94.

7. Koriesh EM, Abo-Soud IH. Facing climate change: urban gardening and sustainable agriculture. Climate Change Impacts on Agriculture and Food Security in Egypt: Land and Water Resources—Smart Farming—Livestock, Fishery, and Aquaculture. 2020:345-419.

8. Hanc A, Novak P, Dvorak M, Habart J, Svehla P. Composition and parameters of household bio-waste in four seasons. Waste Management. 2011;31(7):1450-60.

9. Sumangla H, Malhotra S, Chowdappa P. Urban and Peri-Urban Horticulture—A Perspective. Confederation of Horticulture Associations of India: New Delhi, India. 2013:34.

10. Gilbert OL. The ecology of urban habitats: Springer Science & Business Media; 2012.

11. Beach ES, Cui Z, Anastas PT. Green Chemistry: A design framework for sustainability. Energy & Environmental Science. 2009;2(10):1038-49.

12. Nelson WM. Green solvents for chemistry: perspectives and practice: Oxford University Press; 2003.

13. Horvath IT, Anastas PT. Innovations and green chemistry. Chemical reviews. 2007;107(6):2169-73.

14. Li Y, Chen Y, Wu J. Enhancement of methane production in anaerobic digestion process: A review. Applied energy. 2019;240:120-37.

15. Hobson P, Bousfield S, Summers R, Kirsch E. Anaerobic digestion of organic matter. Critical Reviews in Environmental Science and Technology. 1974;4(1-4):131-91.

16. AliAkbari R, Ghasemi MH, Neekzad N, Kowsari E, Ramakrishna S, Mehrali M, et al. High value add bio-based low-carbon materials: conversion processes and circular economy. Journal of cleaner production. 2021;293:126101.

17. Perey R, Benn S, Agarwal R, Edwards M. The place of waste: Changing business value for the circular economy. Business Strategy and the Environment. 2018;27(5):631-42.

18. Lieder M, Rashid A. Towards circular economy implementation: a comprehensive review in context of manufacturing industry. Journal of cleaner production. 2016;115:36-51.

19. Liu X, Xie Y, Sheng H. Green waste characteristics and sustainable recycling options. Resources, Environment and Sustainability. 2023;11:100098.

20. Koul B, Yakoob M, Shah MP. Agricultural waste management strategies for environmental sustainability. Environmental Research. 2022;206:112285.

21. Rathod SV, Saras P, Gondaliya SM. Environmental pollution: threats and challenges for management. Eco-Restoration of Polluted Environment: CRC Press; 2025. p. 1-34.

22. He B-J, Zhao D-X, Zhu J, Darko A, Gou Z-H. Promoting and implementing urban sustainability in China: An integration of sustainable initiatives at different urban scales. Habitat International. 2018;82:83-93.

23. Ashokkumar V, Flora G, Venkatkarthick R, SenthilKannan K, Kuppam C, Stephy GM, et al. Advanced technologies on the sustainable approaches for conversion of organic waste to valuable bioproducts: Emerging circular bioeconomy perspective. Fuel. 2022;324:124313.

24. Priya K, Rani J, Gwal S. Transforming agricultural residues to value-added products: waste to wealth. Sustainable Management of Agro-Food Waste: Elsevier; 2025. p. 69-85.

25. Fritsche U, Brunori G, Chiaramonti D, Galanakis C, Hellweg S, Matthews R, et al. Future transitions for the bioeconomy towards sustainable development and a climate-neutral economy—knowledge synthesis final report. Publications Office of the European Union, Luxembourg. 2020;10:667966.

26. Sharma R, Malaviya P. Ecosystem services and climate action from a circular bioeconomy perspective. Renewable and sustainable energy reviews. 2023;175:113164.

27. Bishoge OK, Huang X, Zhang L, Ma H, Danyo C. The adaptation of waste-to-energy technologies: Towards the conversion of municipal solid waste into a renewable energy resource. Environmental Reviews. 2019;27(4):435-46.

28. Smith P, Adams J, Beerling DJ, Beringer T, Calvin KV, Fuss S, et al. Land-management options for greenhouse gas removal and their impacts on ecosystem services and the sustainable development goals. Annual Review of Environment and Resources. 2019;44(1):255-86.

29. Duque-Acevedo M, Belmonte-Ureña LJ, Cortés-García FJ, Camacho-Ferre F. Agricultural waste: Review of the evolution, approaches and perspectives on alternative uses. Global Ecology and Conservation. 2020;22:e00902.

30. Peng X, Jiang Y, Chen Z, Osman AI, Farghali M, Rooney DW, et al. Recycling municipal, agricultural and industrial waste into energy, fertilizers, food and construction materials, and economic feasibility: a review. Environmental Chemistry Letters. 2023;21(2):765-801.

31. Panuccio M, Marra F, Maffia A, Mallamaci C, Muscolo A. Recycling of agricultural (orange and olive) bio-wastes into ecofriendly fertilizers for improving soil and garlic quality. Resources, Conservation & Recycling Advances. 2022;15:200083.

32. Shokrollahi S, Denayer JF, Karimi K. Efficient bioenergy recovery from different date palm industrial wastes. Energy. 2023;272:127057.

33. Farhidi F, Madani K, Crichton R. How the US economy and environment can both benefit from composting management. Environmental Health Insights. 2022;16:11786302221128454.

34. Daskalopoulos E, Badr O, Probert S. Economic and environmental evaluations of waste treatment and disposal technologies for municipal solid waste. Applied Energy. 1997;58(4):209-55.

35. Kaniapan S, Hassan S, Ya H, Patma Nesan K, Azeem M. The utilisation of palm oil and oil palm residues and the related challenges as a sustainable alternative in biofuel, bioenergy, and transportation sector: A review. Sustainability. 2021;13(6):3110.

36. Jarrar A, Totti H, Nada H. The potential of palm waste as a source of renewable energy: a case study of Palestine. 2023.

37. Jonoobi M, Shafie M, Shirmohammadli Y, Ashori A, Hosseinabadi HZ, Mekonnen T. A review on date palm tree: Properties, characterization and its potential applications. Journal of Renewable Materials. 2019;7(11):1055-75.

38. Wang J, Azam W. Natural resource scarcity, fossil fuel energy consumption, and total greenhouse gas emissions in top emitting countries. Geoscience Frontiers. 2024;15(2):101757.

39. Kumar R, Strezov V, Weldekidan H, He J, Singh S, Kan T, et al. Lignocellulose biomass pyrolysis for bio-oil production: A review of biomass pre-treatment methods for production of drop-in fuels. Renewable and sustainable energy reviews. 2020;123:109763.

40. Juaidi A, Montoya FG, Ibrik IH, Manzano-Agugliaro F. An overview of renewable energy potential in Palestine. Renewable and Sustainable Energy Reviews. 2016;65:943-60.

41. Jebril A, Khatib I. Bio-energy in Palestine between reality and potential: Lap Lambert Academic Publishing; 2018.

42. Salah WA, Abuhelwa M, Bashir MJ. The key role of sustainable renewable energy technologies in facing shortage of energy supplies in Palestine: Current practice and future potential. Journal of cleaner production. 2021;293:125348.

43. Hechmi S, Zoghlami RI, Mokni-Tlili S, Benzarti S, Moussa M, Jellali S, et al. Agricultural applications. Palm Trees and Fruits Residues: Elsevier; 2023. p. 223-43.

44. Elseify LA, Midani M, Shihata LA, El-Mously H. Review on cellulosic fibers extracted from date palms (Phoenix Dactylifera L.) and their applications. Cellulose. 2019;26:2209-32.

45. Najahi A, Tarrés Q, Delgado-Aguilar M, Putaux J-L, Boufi S. High-Lignin-Containing Cellulose Nanofibrils from Date Palm Waste Produced by Hydrothermal Treatment in the Presence of Maleic Acid. Biomacromolecules. 2023;24(8):3872-86.

46. Henao Rodríguez JE, Escobar Rincón D, Hincapié Rojas DF, Cely Orjuela IG, Socolovsky LM, Erazo Rondón DG, et al. Effects of hydrolysis and bleaching conditions on the efficiency of cellulose microfibrils extraction from coffee parchment through a design of experiments. Cellulose. 2023;30(17):10715-31.

47. Heinze T. Cellulose: structure and properties. Cellulose chemistry and properties: fibers, nanocelluloses and advanced materials. 2016:1-52.

48. Klemm D, Heublein B, Fink HP, Bohn A. Cellulose: fascinating biopolymer and sustainable raw material. Angewandte chemie international edition. 2005;44(22):3358-93.

49. Rao J, Lv Z, Chen G, Peng F. Hemicellulose: Structure, chemical modification, and application. Progress in Polymer Science. 2023;140:101675.

50. Brunner G. Hydrothermal and supercritical water processes: Elsevier; 2014.

51. Hemicellulose [Available from: https://en.wikipedia.org/wiki/Hemicellulose.

52. Muthukumaran P, Kamaraj M, Aravind J, Ramachandran K. Lignin as the most abundant natural polymers as bio-and nanosorbents. Natural Polymers-Based Green Adsorbents for Water Treatment: Elsevier; 2021. p. 111-29.

53. Ez-Zahraoui S, Hassani F-ZSA, El Achaby M, Bouhfid R. Natural fiber reinforcements: classification, extraction, treatment, and properties. Multiscale textile preforms and structures for natural fiber composites: Elsevier; 2023. p. 3-29.

54. Peijs T, Kirschbaum R, Lemstra PJ. Advanced Industrial and Engineering Polymer Research. 2022.

55. Ten E, Vermerris W. Recent developments in polymers derived from industrial lignin. Journal of Applied Polymer Science. 2015;132(24).

56. Ribeiro AM, Santos AI, Veiga F, Figueiras A. Lignin nanoparticle–based nanocomposite hydrogels for biomedical applications. Functional Nanocomposite Hydrogels: Elsevier; 2023. p. 69-90.

57. Tobi AR, Dennis J, Zaid H, Adekoya A, Yar A, Fahad U. Comparative analysis of physiochemical properties of physically activated carbon from palm bio-waste. Journal of Materials Research and Technology. 2019;8(5):3688-95.

58. Britannica. date palm. In: encyclopedia teo, editor. encyclopedia Britannica: Britannica; 2024.

59. Aloud SS, Alharbi HA, Hameed BH, Giesy JP, Almady SS, Alotaibi KD. Production of activated carbon from date palm stones by hydrothermal carbonization and microwave assisted KOH/NaOH mixture activation for dye adsorption. Scientific Reports. 2023;13(1):19064.

60. Mahdi Z, Yu QJ, El Hanandeh A. Removal of lead (II) from aqueous solution using date seed-derived biochar: batch and column studies. Applied Water Science. 2018;8:1-13.

61. Mehrez I, Chandrasekhar K, Kim W, Kim S-H, Kumar G. Comparison of alkali and ionic liquid pretreatment methods on the biochemical methane potential of date palm waste biomass. Bioresource technology. 2022;360:127505.

62. Zhang L, Xu CC, Champagne P. Overview of recent advances in thermo-chemical conversion of biomass. Energy conversion and management. 2010;51(5):969-82.

63. Quan C, Gao N, Song Q. Pyrolysis of biomass components in a TGA and a fixed-bed reactor: Thermochemical behaviors, kinetics, and product characterization. Journal of Analytical and Applied Pyrolysis. 2016;121:84-92.

64. Al-Wabel MI, Ahmad M, Usman AR, Akanji M, Rafique MI. Advances in pyrolytic technologies with improved carbon capture and storage to combat climate change. Environment, climate, plant and vegetation growth. 2020:535-75.

65. Hu X, Gholizadeh M. Biomass pyrolysis: A review of the process development and challenges from initial researches up to the commercialisation stage. Journal of Energy Chemistry. 2019;39:109-43.

66. Balat M. Mechanisms of thermochemical biomass conversion processes. Part 1: reactions of pyrolysis. Energy Sources, Part A. 2008;30(7):620-35.

67. Cheng F, Bayat H, Jena U, Brewer CE. Impact of feedstock composition on pyrolysis of low-cost, protein-and lignin-rich biomass: A review. Journal of Analytical and Applied Pyrolysis. 2020;147:104780.

68. Laiq Ur Rehman M, Iqbal A, Chang CC, Li W, Ju M. Anaerobic digestion. Water Environment Research. 2019;91(10):1253-71.

69. Balan V, Bals B, Chundawat SP, Marshall D, Dale BE. Lignocellulosic biomass pretreatment using AFEX. Biofuels: methods and protocols. 2009:61-77.

70. Lau MJ, Lau MW, Gunawan C, Dale BE. Ammonia fiber expansion (AFEX) pretreatment, enzymatic hydrolysis, and fermentation on empty palm fruit bunch fiber (EPFBF) for cellulosic ethanol production. Applied biochemistry and biotechnology. 2010;162:1847-57.

71. Qiao X, Zhao C, Shao Q, Hassan M. Structural characterization of corn stover lignin after hydrogen peroxide presoaking prior to ammonia fiber expansion pretreatment. Energy & fuels. 2018;32(5):6022-30.

72. Hoover AN, Tumuluru JS, Teymouri F, Moore J, Gresham G. Effect of pelleting process variables on physical properties and sugar yields of ammonia fiber expansion pretreated corn stover. Bioresource technology. 2014;164:128-35.

73. Passetti RA, Passetti LC, Gruninger RJ, Ribeiro GO, Milani MRM, Prado IN, et al. Effect of ammonia fibre expansion (AFEX) treatment of rice straw on in situ digestibility, microbial colonization, acetamide levels and growth performance of lambs. Animal Feed Science and Technology. 2020;261:114411.

74. Klemm D, Cranston ED, Fischer D, Gama M, Kedzior SA, Kralisch D, et al. Nanocellulose as a natural source for groundbreaking applications in materials science: Today’s state. Materials Today. 2018;21(7):720-48.

75. Melhem AMR. Synthesis and characterization of magnetic nano cellulose from olive waste (Jeft) for the effective removal of methylene blue from water: An-Najah National University; 2017.

76. Sabaruddin FA, Paridah M, Sapuan S, Ilyas R, Lee SH, Abdan K, et al. The effects of unbleached and bleached nanocellulose on the thermal and flammability of polypropylene-reinforced kenaf core hybrid polymer bionanocomposites. Polymers. 2020;13(1):116.

77. Trache D, Tarchoun AF, Derradji M, Hamidon TS, Masruchin N, Brosse N, et al. Nanocellulose: from fundamentals to advanced applications. Frontiers in Chemistry. 2020;8:392.

78. Deepa B, Abraham E, Cordeiro N, Mozetic M, Mathew AP, Oksman K, et al. Utilization of various lignocellulosic biomass for the production of nanocellulose: a comparative study. Cellulose. 2015;22:1075-90.

79. Nor Fazelin M, Salma Mohamad Yusop SMY, Ishak Ahmad IA. Preparation and characterization of cellulose and nanocellulose from pomelo (Citrus grandis) albedo. 2015.

80. Hop TTT, Mai DT, Cong TD, Nhi TTY, Loi VD, Huong NTM, et al. A comprehensive study on preparation of nanocellulose from bleached wood pulps by TEMPO-mediated oxidation. Results in Chemistry. 2022;4:100540.

81. Jodeh S, Hamed O, Melhem A, Salghi R, Jodeh D, Azzaoui K, et al. Magnetic nanocellulose from olive industry solid waste for the effective removal of methylene blue from wastewater. Environmental science and pollution research. 2018;25:22060-74.

82. Parameshwaran R, Sarı A, Jalaiah N, Karunakaran R. Applications of thermal analysis to the study of phase-change materials. Handbook of thermal analysis and calorimetry. 6: Elsevier; 2018. p. 519-72.

83. Emiola-Sadiq T, Zhang L, Dalai AK. Thermal and kinetic studies on biomass degradation via thermogravimetric analysis: a combination of model-fitting and model-free approach. ACS omega. 2021;6(34):22233-47.

84. Jain AA, Mehra A, Ranade VV. Processing of TGA data: Analysis of isoconversional and model fitting methods. Fuel. 2016;165:490-8.

85. Mishra RK, Mohanty K. Pyrolysis kinetics and thermal behavior of waste sawdust biomass using thermogravimetric analysis. Bioresource technology. 2018;251:63-74.

86. Tanzi MC, Farè S, Candiani G. Foundations of biomaterials engineering: Academic Press; 2019.

87. Prime RB, Bair HE, Vyazovkin S, Gallagher PK, Riga A. Thermogravimetric analysis (TGA). Thermal analysis of polymers: Fundamentals and applications. 2009:241-317.

88. De Blasio C, De Blasio C. Thermogravimetric analysis (TGA). Fundamentals of Biofuels Engineering and Technology. 2019:91-102.

89. Feller S. Density, Thermal Properties, and the Glass Transition Temperature Ofglasses. Modern glass characterization. 2015:1-31.

90. Thermogravimetric Analysis [Available from: https://millwiki.mse.gatech.edu/index.php?title=Thermogravimetric_Analysis.

91. Loganathan S, Valapa RB, Mishra RK, Pugazhenthi G, Thomas S. Thermogravimetric analysis for characterization of nanomaterials. Thermal and rheological measurement techniques for nanomaterials characterization: Elsevier; 2017. p. 67-108.

92. Ebnesajjad S. Surface and material characterization techniques. Handbook of adhesives and surface preparation: Elsevier; 2011. p. 31-48.

93. Yuan X, He T, Cao H, Yuan Q. Cattle manure pyrolysis process: kinetic and thermodynamic analysis with isoconversional methods. Renewable Energy. 2017;107:489-96.

94. Riyaz NS, Badran I. The catalytic thermo-oxidative decomposition of glimepiride using the isoconversional method. Journal of Thermal Analysis and Calorimetry. 2022;147(19):10755-65.

95. Vyazovkin S. Isoconversional kinetics of thermally stimulated processes: Springer; 2015.

96. Badran I, Manasrah AD, Hassan A, Nassar NN. Kinetic study of the thermo-oxidative decomposition of metformin by isoconversional and theoretical methods. Thermochimica Acta. 2020;694:178797.

97. Nie N, Wang Y, Yellezuome D, Liu X, Wang P, Wang X, et al. Exploring kinetic and thermodynamic mechanisms of switchgrass pyrolysis using iterative linear integral isoconversional method and master plots approach. Fuel. 2023;338:127266.

98. Rong X, Huang Q. Calorimetric analysis. In: Goss MJ, Oliver M, editors. Encyclopedia of Soils in the Environment (Second Edition). Oxford: Academic Press; 2023. p. 662-9.

99. Demarest SJ, Frasca V. Differential scanning calorimetry in the biopharmaceutical sciences. Biophysical characterization of proteins in developing biopharmaceuticals: Elsevier; 2020. p. 311-32.

100. Ghanbari E, Picken SJ, van Esch JH. Analysis of differential scanning calorimetry (DSC): determining the transition temperatures, and enthalpy and heat capacity changes in multicomponent systems by analytical model fitting. Journal of Thermal Analysis and Calorimetry. 2023;148(22):12393-409.

101. Hamed OA, Jodeh S, Al-Hajj N, Hamed EM, Abo-Obeid A, Fouad Y. Cellulose acetate from biomass waste of olive industry. Journal of wood science. 2015;61:45-52.

102. buchiglasuster bmd 300 [Available from: https://www.buchiglas.com/en/pressure-reactors-stirred-autoclaves/magnetic-couplings.html.

103. Avci U, Zhou X, Pattathil S, da Costa Sousa L, Hahn MG, Dale B, et al. Effects of extractive ammonia pretreatment on the ultrastructure and glycan composition of corn stover. Frontiers in Energy Research. 2019;7:85.

104. Montgomery DC. Design and analysis of experiments: John wiley & sons; 2017.

105. Customized TGA Vacuum and Atmosphere Controlled Tube Furnace optional 1200 - 1700C - OTF-X-TGA [Available from: https://www.premier-

sols.com/partners/item/customized-tga-vacuum-and-atmosphere-controlled-tube-furnace-optional-1200-1700c-otf-x-tga.html.

106.SANAF TGA device [Available from: https://sanaf.com/tga/.

107.Origin. Scientific Data Analysis and Graphing Software. Version 2024. OriginLab; 2024

[Available from: URL: ww.OriginLab.com.

108.Atkins PW, De Paula J, Keeler J. Atkins' physical chemistry: Oxford university press; 2023.

109.The Discovery SDT 650 device [Available from: https://www.tainstruments.com/sdt-650/.

110.Badran I, Hassan A, Manasrah AD, Nassar NN. Experimental and theoretical studies on the thermal decomposition of metformin. Journal of Thermal Analysis and Calorimetry. 2019;138:433-41.

111.Badran I, Rauk A, Shi Y. Theoretical study on the ring-opening of 1, 3-disilacyclobutane and H2 elimination. The Journal of Physical Chemistry A. 2012;116(48):11806-16.

112.Cole-Parmer. (n.d.). Thermo Scientific Nicolet iD3 ZnSe ATR for the Nicolet iS5 FT-IR Spectrometer. [Available from: https://www.coleparmer.co.uk/i/thermo-scientific-nicolet-869-142300-id3-znse-atr-for-the-nicolet-is5-ft-ir-spectrometer/8300822.

113.Drašar P. John E. McMurry: Organic Chemistry. Chemické listy. 2011;105(9):713-.

114.FEI Company. (n.d.). Nova Nano SEM 450. [Available from: https://www.thermofisher.com/ps/en/home.html.

115.Abd Mutalib M, Rahman M, Othman M, Ismail A, Jaafar J. Scanning electron microscopy (SEM) and energy-dispersive X-ray (EDX) spectroscopy. Membrane characterization: Elsevier; 2017. p. 161-79.

116. Saif T, Lin Q, Butcher AR, Bijeljic B, Blunt MJ. Multi-scale multi-dimensional microstructure imaging of oil shale pyrolysis using X-ray micro-tomography, automated ultra-high resolution SEM, MAPS Mineralogy and FIB-SEM. Applied energy. 2017;202:628-47.

117. Rayung M, Ibrahim NA, Zainuddin N, Saad WZ, Razak NIA, Chieng BW. The effect of fiber bleaching treatment on the properties of poly (lactic acid)/oil palm empty fruit bunch fiber composites. International journal of molecular sciences. 2014;15(8):14728-42.

118. Ching YC, Ng TS. Effect of preparation conditions on cellulose from oil palm empty fruit bunch fiber. BioResources. 2014;9(4):6373-85.

119. Kian L, Saba N, Jawaid M, Alothman O, Fouad H. Properties and characteristics of nanocrystalline cellulose isolated from olive fiber. Carbohydrate polymers. 2020;241:116423.

120. Carrier M, Loppinet-Serani A, Denux D, Lasnier J-M, Ham-Pichavant F, Cansell F, et al. Thermogravimetric analysis as a new method to determine the lignocellulosic composition of biomass. Biomass and bioenergy. 2011;35(1):298-307.

جــامعـــة النجاح الوطنية

كليـــة الدراســـات العليـــا

دراسة التحلل التأكسدي الحراري لمخلفات النخيل باستخدام الخواص الحركية المتقاربة وتكنولوجيا توسع ألياف الأمونيا

إعداد

ضحى عبد الله فتحي يوسف

إشراف

د. إسماعيل بدران

د. ضرار صمادي

قدمت هذه الرسالة استكمالا لمتطلبات الحصول على درجة الماجستير في الكيمياء، من كلية الدراسات العليا، في جامعة النجاح الوطنية، نابلس– فلسطين.

2025

دراسة التحلل التأكسدي الحراري لمخلفات النخيل باستخدام الخواص الحركية المتقاربة وتكنولوجيا توسع ألياف الأمونيا

إعداد

ضحى عبد الله فتحي يوسف

إشراف

د. إسماعيل بدران

د. ضرار صمادي

الملخص

تتناول هذه الدراسة حركية التحلل الحراري للأوراق النخيل الخام والمعالجة كيميائيا باستخدام التبييض (المبيضة) باستخدام التحليل الحراري الوزني لقياس فقدان الكتلة أثناء التسخين، وتقنية المسح الحراري التفاضلي لتحديد التغيرات في الطاقة الحرارية أثناء التحلل، بالإضافة إلى استخدام طرق الخواص الحركية المتقاربة مثل طرق فريدمان وكيسنجر–أكاهير–سونو. من النتائج المستخلصة من التحليل الحراري الوزني، تم ملاحظة أنماط تحلل حراري واضحة في جو أكسيدي، حيث تحللت أوراق النخيل الخام ضمن نطاق درجة حرارة 215–565 درجة مئوية، بينما تحللت أوراق النخيل المبيضة بين 200–490 درجة مئوية. تؤدي عملية التبييض الكيميائي إلى تقليل الاستقرار الحراري للمادة، وذلك بسبب إزالة اللجنين والهيميسليلوز ، مما يجعلها أكثر ملاءمة لتطبيقات الطاقة الحيوية.

تم إجراء التحليل الحركي باستخدام طريقتي فريدمان وكيسنجر–أكاهيرا–سونو لتحديد تأثير عملية التبييض. أدى التبييض إلى تقليل طاقة التنشيط، مما أدى إلى تسريع عملية التحلل. على النقيض من ذلك، ظهرت طريقة فريدمان نطاقًا واسعًا من قيم طاقة التنشيط (300–440 كيلوجول/مول)، مما يدل على وجود آليات تفاعل متعددة ومعقدة في العينات المبيضة، بينما أظهرت طريقة كيسنجر–أكاهيرا–سونو قيمًا أكثر استقرارًا لطاقة التنشيط، حيث تراوحت ضمن نطاق ضيق (140–190 كيلوجول/مول)، مما يعكس آليات تفاعل أبسط.

أظهرت نتائج تحليل المسح الحراري التفاضلي أن زيادة معدل التسخين أدت إلى ارتفاع درجة حرارة التحلل وإجمالي الطاقة المنبعثة. كما تبين أن العينات المبيضة أطلقت طاقة أكبر أثناء التحلل الحراري (3411.33 وحدة تقديرية عند 25 درجة مئوية/دقيقة) مقارنة بالعينات الخام (3107.67 وحدة تقديرية). يشير هذا إلى أن المعالجة الكيميائية، مثل التبييض، تلعب دورًا مهمًا في تحسين كفاءة التحلل، وذلك من خلال تعديل البنية الكيميائية للمادة وزيادة قابليتها للتفكك الحراري.

أظهرت نتائج النمذجة الحركية اختلافًا إحصائيًا في قيم العامل المسبق (A_α) وانتروبيا التنشيط ($\Delta S^{\neq}$) بين الأوراق الخام والمبيضة. فعند نسبة تحويل 25% (α=0.25)، كانت قيم A_α في الأوراق الخام أعلى حيث بلغت 1.4×10^{30} ثانية$^{-1}$، مقارنة بالقيم المسجلة في العينات المبيضة والتي وصلت إلى 1.4×10^{26} ثانية$^{-1}$. كما أظهرت الأوراق الخام $\Delta S^{\neq}$ أعلى (318.5 جول/مول. كلفن) مقارنة بالعينات المبيضة (241.9 جول/مول.كلفن)، مما يدل على أن المادة الخام تمتلك تركيبة أكثر تعقيدًا من حيث الروابط الكيميائية، مما يسبب فوضى جزيئية أكبر أثناء التفاعل، وهو ما يتطلب طاقة أكبر لبدء التفاعل.

كشفت المعلمات الديناميكية الحرارية أن تحلل الأوراق الخام يتطلب حرارة تنشيط أعلى ($\Delta H^{\neq}$ = 351.9 كيلوجول/مول) مقارنة بالعينات المبيضة ($\Delta H^{\neq}$ = 299.6 كيلوجول/مول)، مما يشير إلى أن عملية تحلل الأوراق الخام تحتاج إلى طاقة أكبر، مما يجعلها أقل قابلية للتحلل مقارنة بالعينات المبيضة.

أظهرت نتائج تحليل طيف الأشعة تحت الحمراء أن عملية التبييض أدت إلى تغيرات في التركيب الكيميائي للمادة، حيث تم ازالة محتوى اللجنين والهيميسليلوز، مما جعل البنية الجزيئية للمادة أكثر تبسيطًا وأقل تعقيدًا.

كلمات مفتاحية: سعف النخيل؛ تمدد ألياف الأمونيا؛ عملية التبييض؛ التحليل الحراري الثيرموغرافي، المسح الحراري التفاضلي؛ طرق التحويل المتساوي؛ إنتاج الطاقة الحيوية؛ الاستقرار الحراري؛ البارامترات الحركية